PHENOTYPIC SIGNATURES AND MOLECULAR MECHANISMS OF CANCER CELL INVASION

by
Angela C. San

A thesis submitted to Johns Hopkins University in conformity with the requirements for the degree of Master of Science in Engineering

Baltimore, Maryland
May, 2014

ABSTRACT

The leading cause of cancer-related deaths is when cancer progresses to the metastatic stage, spreading into secondary sites. In order to combat metastasis, emerging research in cancer biology examines signaling pathways and mechanisms that are involved in the malignant transformation of cancer cells. An early stage in metastasis is invasion, where cells detach from their original environment and invade into surrounding tissue. Despite the significance of cell invasion, a complete picture of how invasion takes place is lacking, partially due to the limitations of complicated, time consuming, and costly platforms currently used to study this process.

In this thesis, we utilized a 2.5D assay that combines the ease of 2D cell culture techniques with the physiological relevance of the 3D environment. Cells were first plated and allowed to spread on collagen coated 2D substrates, followed by the casting of 1 μm-thick 3D collagen gels on top of the cells. Unlike other invasion assays, this platform features a clearly defined 2.5D interface between the substrate and gel, which allowed high-resolution imaging of the morphological transition of cells from 2D to 3D and accurate quantification of the fraction of cells that invaded into the gel. Moreover, data collection and analysis do not require highly technical machinery or software.

The novel functions of our assay led us to discover that cells instantaneously form microspikes that outline the entire cell body (within two hours after collagen gel casting) that may play a role in invasion. We further investigated the factors that influence invasion and discovered that the invasion of fibrosarcoma HT1080 cells is due to active cellular processes rather than simple diffusion and do not depend on matrix concentration or substrate rigidity. However, at low concentrations of collagen, HT1080 cells can

invade independent of actomyosin proteins, cell-ECM binding, and the degradation of the surrounding tissue. Furthermore, we investigated the potential similarities of microspikes to filopodia and their involvement in invasion. Our preliminary results revealed that the depletion of filopodia-related proteins had no effects on microspike formation or invasion. Through examining various cell lines, we were able to establish a positive correlation between the quantity of microspikes formed and invasion capabilities, which can be used as a tool to quickly predict whether a cell line can invade from 2D substrates to 3D matrices. Finally, the phenomenon observed in this system defies durotaxis; the movement of cells from a stiff substrate to a softer gel is a novel discovery.

Our system allows analysis at high resolution to observe changes at the single cell level as well as accurately quantify invasion percentages at the larger scale. This system can be used to delve deeper into the connection between the formation of microspikes and invasion, potentially uncovering the elusive first steps of invasion. The advantages that this novel assay provides over current methodologies can act as a solution to the drawbacks of current invasion studies. Furthermore, it can serve as an example for the design of future invasion assays that will be high throughput, low cost, and accessible.

ACKNOWLEDGEMENTS

I would like to thank everyone for their guidance and support throughout my time in the Wirtz Lab to pursue my Masters of Science in Chemical and Biomolecular Engineering. I would first like to thank Dr. Wirtz for being my mentor and advisor ever since I was a freshman at Johns Hopkins. Throughout my graduate studies, his constant enthusiasm and valuable input has really helped me grow as an engineer and a researcher. His devotion to his work has inspired me to always continue learning and to remain passionate about my interests. I also would like to thank Dr. Konstantopoulos for being a member of my thesis committee and for his input on this work. I am really grateful for his contributions, time, and effort. I would also like to thank Dr. Lijuan He who has also been such a wonderful mentor to me. It has been a pleasure to work with her on this project and learn from such a talented scientist. She has truly taught me an incredible amount about research and also academically stimulated me to excel to the best of my abilities. In addition, I would also like to thank everyone in the Wirtz lab for their encouragement; it has been such a great experience to work alongside these intelligent scientists who have such bright futures ahead of them. Finally, I would like to acknowledge my family and friends for their endless love and support throughout my studies. They have motivated me every step of the way, and I would not have accomplished this work without them.

TABLE OF CONTENTS

DEFINITION OF SYMBOLS

CIA	Circular invasion assay
ECM	Extracellular Matrix
EMT	Epithelial to Mesenchymal Transition
FERM	4.1/ezrin/radixin/moesin
FLP	Filopodia like protrusions
KD	Knock down
LatB	Latrunculin B
MMP	Matrix Metalloproteinase
MMT1-MMP	Membrane-Type 1 Matrix Metalloproteinase
PAA	Polyacrylamide
WT	Wild type

LIST OF FIGURES

INTRODUCTION

Metastasis is the leading cause of death from cancer and is responsible for 90% of cancer-related deaths (Mierke et al., 2013). In most cases, the primary tumor can be surgically removed and is not the clinical problem of cancer. However, the dissemination of these malignant cells results in difficulty of treatment and ultimately death (Nürnberg et al., 2011). Cancer treatment began using harsh methods such as radiotherapy and chemotherapy to kill cells that uncontrollably proliferate; however, these methods could not differentiate the healthy cells that surrounded the sick cells. The focus progressed to studying the causes of the cancer by targeting the signaling pathways of cells that deviate from its normal processes to malignancy (Zimmerman et al., 2013).

One of the initial steps of metastasis is invasion of cancer cells from the diseased organ into the local tissue, which includes changes in tumor cell adherence to neighboring cells and the extracellular matrix (ECM), remodeling of the ECM, and the physical movement of a tumor cell through the tissue (Steeg 2006). Invasive behavior requires the reorganization and reassembly of the actin cytoskeleton, such as the dissolution of cell-cell contacts, formation of protrusions, and the creation of force to migrate through the surrounding tissue (Nürnberg et al., 2011). Since invasion is an early step in metastasis, understanding the signaling mechanisms underlying this prerequisite can help prevent cells from spreading to a secondary site. Unfortunately, if tumor formation is not caught in time, intravasation of tumor cells into the bloodstream, survival and migration through blood vessels, extravasation into a distant tissue, and colonization in a secondary site can occur (Nguyen et al., 2009) (See Figure 1).

Clinically, this translates into increased seriousness of the disease and difficulty in treatment of the systemic disease, resulting in higher mortality rates. (Steeg 2006).

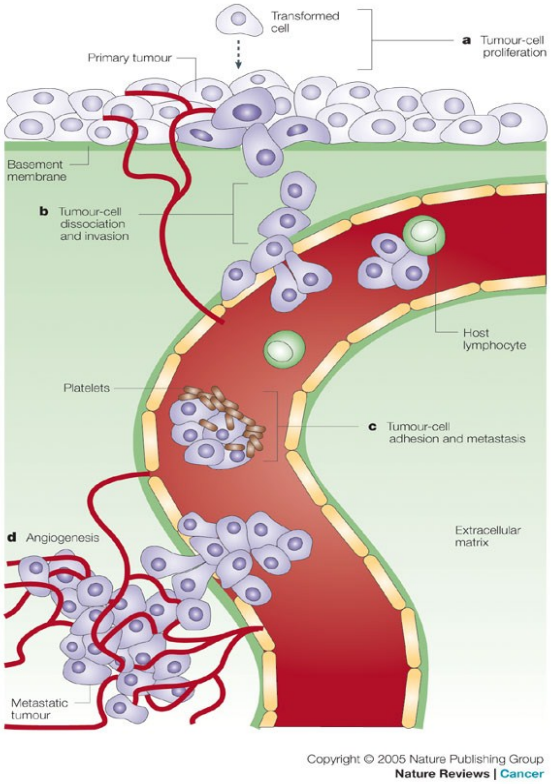

Figure 1: Schematic of Metastasis. **(A)** Proliferation of tumor cells with transformed adhesive properties to their neighboring cells and their surrounding environment. **(B)** Tumor cells dissociate from other tumor cells and invade through the basement membrane into the extracellular matrix. **(C)** The cells then enter the blood stream and travel to a distant site via circulation. **(D)** After exiting the blood stream, tumor cells colonize into a secondary tumor and survive through processes like angiogenesis (Fuster et al., 2005).

Invasion modes of tumor cells fall into three major categories that vary according to tumor type and its microenvironment; these include mesenchymal invasion, amoeboid

invasion, and collective migration. Mesenchymal invasion, the best understood mode, occurs when 10% to 40% of carcinomas experience an epithelial to mesenchymal transition (EMT) (Sahai et al., 2005). Cells undergo continued changes in gene expression and obtain an elongated morphology, while losing cell-cell adhesions. Recent discoveries have revealed that cancer cells detaching from the primary tumor and invading into surrounding tissues resembles EMT in biomechanical, cellular and molecular levels (Mierke et al., 2011). Amoeboid motility is characterized by rounded cell shape that uses high contractility to squeeze through the ECM without requiring extracellular proteolysis. Finally, collective motility occurs when whole sheets of cells with intact cell-cell adhesions migrate by proteolytic degradation of the ECM (Sahai et al., 2005) (Nürnberg et al., 2011).

Actin-based protrusions sense the environment before invasion

Before invasion, cells first probe their environment at the cell front. Three types of actin-based protrusive structures at the leading edge of the cell are lamellipodia, filopodia, and invadopodia. Actin is a monomeric protein that polymerizes into polarized filaments with a fast-growing barbed end, where new actin subunits bind, and a much slower growing minus end (Cooper et al., 2009) (Griffth et al., 2011). Lamellipodia are broad, thin, sheet-like regions that are composed of branched networks of actin filaments, whereas filopodia are tightly bundled parallel actin filaments. Invadapodia are actin-based protrusions that proteolytically degrade the ECM, formed particularly to help cells invade the basement membrane (Ridley 2011). Since these structures degrade the extracellular matrix, they require the presence of matrix-degrading proteases (Yu et al.,

2012). All types of protrusions use actin polymerization to push the cell forward in migration and have complex signaling pathways that need to be functioning correctly at every step in order for important cellular processes like cell adhesion, migration, or angiogenesis to occur (Ridley 2011).

The primary known role of filopodia is to explore its local environment for cues. The barbed ends of the actin filaments are pointed towards the plasma membrane so that myosin X, an unconventional motor protein with FERM (4.1/ezrin/radixin/moesin) binding domains, can transport cargoes to the tips of filopodia. Integrins, heterodimeric transmembrane proteins, are one of the cargoes that bind to the FERM domain and are localized at the tips to transmit signals from the cytoskeleton to the surrounding microenvironment. Integrins are extremely important in invasion because they regulate cell-matrix adhesion, deadhesion, adhesion strength, and outside-in signaling through binding ligands in the ECM (Mierke et al., 2011). Currently, it is not known whether the integrins present in the filopodia can participate in outside-in signaling (Steeg 2006) (Arjonen et al., 2011). The motor-domain of myosin X can induce filopodia formation without integrin binding to substrates; however, filopodia formation with integrin mediated attachment are longer and more stable compared to those without integrin (Cheney et al., 2006) (Arjonen et al., 2011).

The stability of filopodia is regulated by fascin, a crosslinking protein that tightly bundles actin filaments, providing the stiffness required to efficiently push the membrane (Vignjevic et al, 2006). Fascin is strongly implicated in cancer progression and is upregulated at the invasive cell front. Even though the interaction of fascin with actin bundles is highly dynamic, upregulation of fascin increases motility in both normal and

cancer cells. In non-small cell lung cancer and breast cancer, high expression of fascin has been correlated with an increased risk of invasion. Additionally, in human colon cancer, fascin was expressed at the invasive front and promoted metastasis (Matilla et al., 2008). Hypothetically, these poor prognoses are because of fascin's role in bundling actin protrusion and its regulatory role in formation of invadopodia (Mattilla et al., 2008) (Arnojen et al., 2011). Another important upstream molecule involved in filopodia formation is cdc42, which was the first Rho GTPase found to promote the formation of filopodia (Ridley 2011) (Matilla et al., 2008). This molecule has the power to summon molecules required for filopodia initiation and extension (Ridley 2011) (See Figure 2).

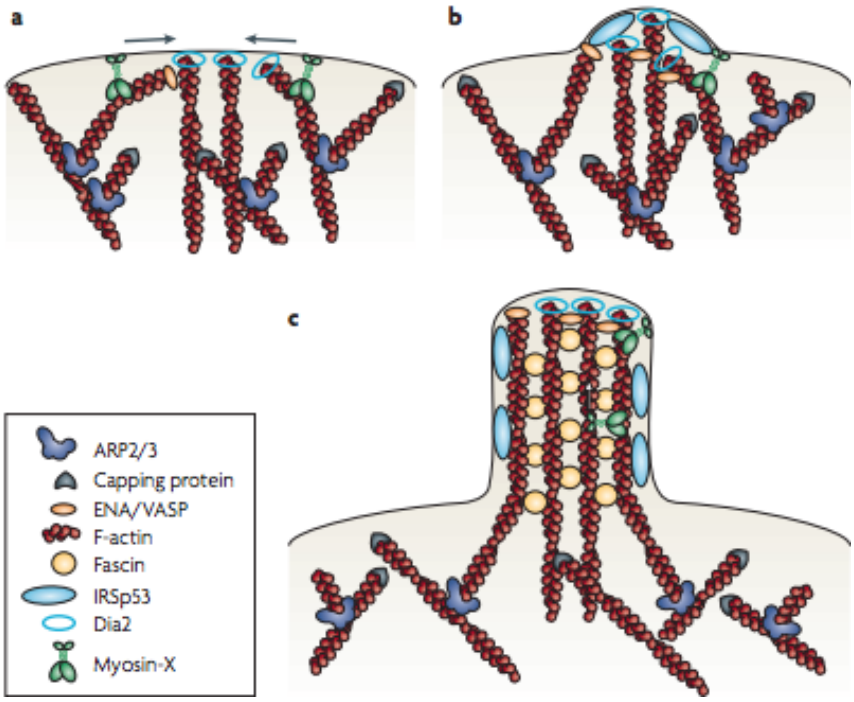

Figure 2: Proteins involved in filopodia formation. **(A)** The barbed ends of the actin filaments converge together through the motor activity of myosin X, intiating the formation of a filopodium. **(B)** Cdc42 brings together IRSp53, ENA/VASP, and Dia2, which all contribute to the intiation of the filopodium. IRSp53 may further help create

plasma membrane protrusion, while ENA/VASP proteins can act as temporary actin-crosslinking proteins at the tip of a growing filament. **(C)** Fascin crosslinks at the shaft of the filopodium and stabilizes the bundle. At this point, myosin X molecules may transport adhesion proteins, such as integrin, to the barbed ends of the filopodia (Matilla et al., 2008).

Process overview of invasion

Previous research of cells on both 2D substrates and in vitro invasion assays have provided us pieces of information regarding cell invasion and migration, which comprises of reorganization of the actin cytoskeleton to generate traction and degradation of the ECM to provide cells the room to invade (Matilla et al., 2008) (Friedl et al., 2007). Filopodia, which originate from the lamellipodia, explore the environment. The integrins that localize in filopodia are in an activated but unbound state, signifying that they are prepared to explore the surrounding environment. After receiving information from filopodia's receptors to signal molecules and ECM molecules, these thin structures form initial adhesion sites. To strengthen this attachment, focal adhesion complex components are summoned and form mature focal adhesions. Eventually, the cytoskeleton reorganizes to actin stress fibers, and filopodia transform into lamellipodia-like protrusions (Mattila et al., 2008) (Guillou et al., 2008). In the final steps of cell migration, the nucleus and cell body are moved forward by actomyosin-based contraction forces, and retraction forces move the rear of the cell forward by dissembling adhesions in the trailing edge of the cell (Mattila et al., 2008) (See Figure 3).

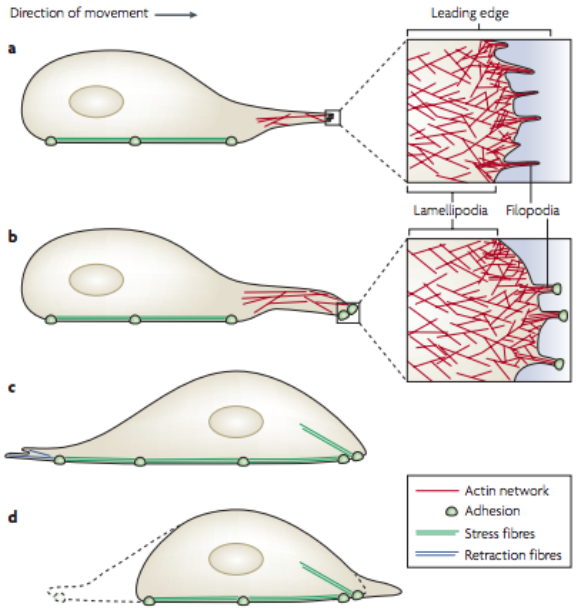

Figure 3: Steps of cell motility**. (A)** The cell is sensing its environment through the formation of actin-dense lamellipodia and filopodia. **(B)** After the cell decides upon a direction, it uses integrin to connect to the ECM to form focal adhesions. **(C)** Stress fibers start to pull the cell body and nucleus forward. **(D)** The back end of the cell retracts and dissociates any adherences to follow the rest of the cell body (Matilla et al., 2008).

Once the cell has geared its machinery to invade, metalloproteinases (MMPs), required in two out of the three modes of invasion, come into play. These cell surface proteins, such as MT1-MMP, degrade the ECM through contact-dependent proteolysis and structurally remodel the connective tissue to form gaps in the matrix (Friedl et al., 2007). As well as degrading the ECM, secreted MMPs can cleave growth-factor binding proteins, growth factor precursors, receptor tyrosine kinases, cell-adhesion molecules, and other proteinases (Chambers 1997) (Friedl et al., 2007). Their expression and activation is upregulated in almost all human cancers relative to normal tissue and correlated with poor survival (Mierke et al., 2011). MMPs can further cancer progression

by increasing functions such as cancer-cell growth, migration, invasion, metastasis and angiogenesis (Egeblad 2002).

The relationship between cancerous cells and the extracellular matrix

The ECM is composed of many proteins, such as collagen, fibronectin, laminin, and hyaluronan, which are mostly secreted by fibroblasts (Alberts 2008). Type I collagen maintains the structure of most interstitial tissues and organs such as the skin, gut, and breast; it also functions as a structural scaffold, controls stiffness, resists tension, binds adhesion factors, binds growth factors, and is porous (Griffith et al., 2006). The basement membrane, a thin mesh of proteins, blocks cells from invading into the surrounding tissue (Alberts 2008).

The physical properties of the ECM were shown to significantly affect the behavior of cells in its proximity. For example, the tumor microenvironment depends on matrix stiffness, pore-size, crosslinking points, crosslinking proteins, thickness, extracellular matrix fiber network composition, and orientation (Mierke et al., 2011). The stiffness of the matrix and the concentration of bonds formed between integrin and the microenvironment affect how strongly the cells can contract the matrix and how easily the cells can migrate through the ECM (See Figure 4). The rigidity of a substrate, which is defined by the elastic modulus, controls cellular growth, differentiation and other functions in a wide variety of cell types (Lo et al., 2000). A more rigid substrate increases the proliferation in non-tumorigenic mammary epithelial cells and decrease E-cadherin expression, which regulates cell-cell adhesion. Over time, the ECM is stiffer near a primary tumor than near healthy cells due to denser, more crosslinked collagen;

this can dictate the behavior of cancer cells by promoting the selection of aggressive, highly invasive cancer cell, which possess the mutated genes that can help overcome the remodeled ECM (Mierke et al., 2011).

As cancer cells invade into the ECM, they have the capability to alter the composition of its surrounding environment to allow for single or collective cell invasion (Griffith et al., 2006). Cells *in vivo* can bundle collagen fibers through generating contractile forces using their protrusions, leading to more surface areas for larger focal adhesions to form, which may play a role in invasion. 3D traction microscopy further showed that cells not only pull on the collagen fibers in their local environment, but also exhibit activated MMPs (Mierke et al., 2013) (Egeblad 2002). Upregulated MMPs proteolytically degrade the ECM and create micro- and macrotracks that are surrounded by condensed collagen fibers. These tracks guide tumor cells through the tissue, widen from pressure by the invading cells, and ultimately promote cancer invasion (Friedl et al., 2011). Along with altering the properties of the ECM, cells respond to many soluble signals in the ECM; these signals exist in a concentration gradient, such as growth factors and effector molecules (Griffith et al., 2006). It has been hypothesized that as cancer progresses, the ability of cancer cells to sense the properties of the microenvironment increases (Mierke et al., 2011).

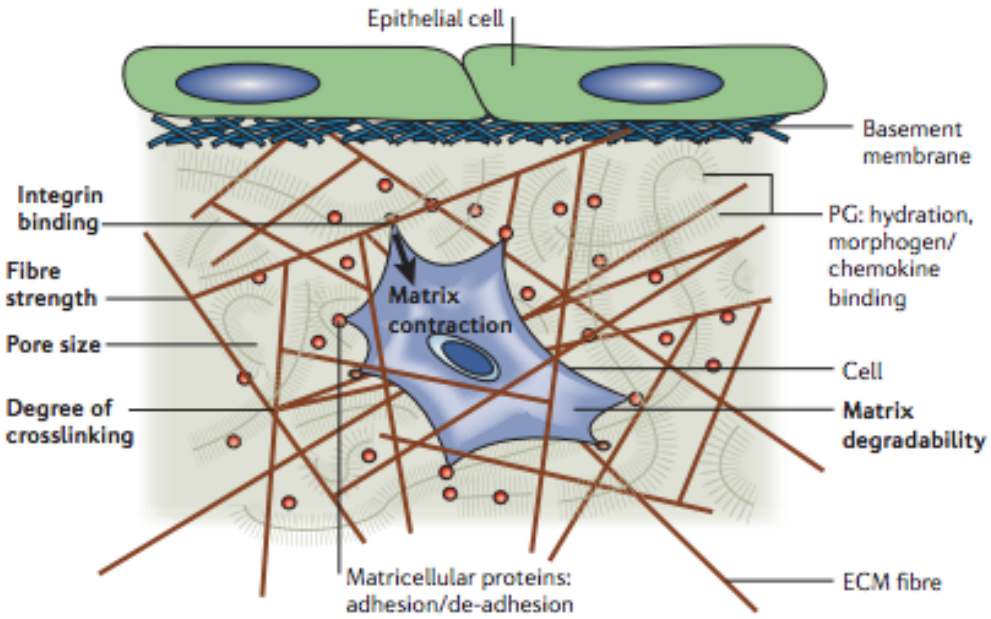

Figure 4: Parameters of the Extracellular Matrix. Epithelial cells sit on top of the basement membrane and the ECM. A fibroblast cell is depicted in the midst of the ECM, its usual environment. Many important variables of the ECM are shown in this figure, such as integrin binding, pore size, degree of crosslinking, and matrix degradability (Griffith et al., 2006).

Common three-dimensional matrices used in in vitro testing

Recently, there is an increasing demand for *in vitro* models to mimic the ECM's complexity in more relevant methods than traditional 2D petri dishes. Most cells require signals from a three-dimensional (3D) environment to form physiological tissue structures *in vitro* and behave more similarly as it would *in vivo* (Griffth et al., 2006). 3D models add another dimension for cellular adhesion and external factors. The usage of 3D cell culture also introduces a new dimension in cell-based assays that can identify drugs that would not have any significance in 2D cultures (Felder et al., 2008). For example, in the breast cancer cell line MDA-MB-231, 3D testing has revealed that its

invasion is dependent on collective migration, involving inhibitors that are effective in 3D but have negative results in 2D assays. In HT1080, a fibrosarcoma cell line, mesenchymal-amoeboid transition in motility is observed with MMPi treatment. Invasion of these cells in 3D and *in vivo* is resistant to MMPi but is affected in 2D environments (Zimmerman et al., 2013) (Eccles et al., 2005). A way to capture the physiology of the ECM is to use molecules found in the ECM.

The first novel gel to try and mimic the ECM is the 2D system of polyacrylamide (PAA) gels to analyze cell responses due to the change in substrate stiffness below the cells. This PAA gel provides conditions of controlled adhesion-receptor ligation and is highly resistant to protein adsorption and relatively resistant to changes due to the cell. The elastic modulus can be tuned from 100 to 10,000 Pa by varying the ratio of monomer to crosslinkers, which can affect a wide range of cells. PAA gels are used to provide a link between the matrix stiffness and cell phenotype. (Griffth et al, 2006).

Type I collagen is a commonly used natural ECM gel that is easily accessible and can provide the chemical and physical properties that elicit physiological cell function and morphology, both of which can polymerize and form a 3D gel under the right conditions (Even-Ram et al., 2005). *In vitro*, it is found as reconstituted type I collagen, commonly extracted and processed from rat tail (Wolf et al., 2009). A disadvantage of using natural ECMs is that the gels can be heterogeneous in their composition and mechanical properties due to production variability (Felder et al., 2009). To overcome these shortcomings, collagen can be found in a synthetic form of electrospun polymer fibers or fibril-forming peptides that produce specific ECM properties that are well controlled and reproducible *in vitro* (Griffth et al., 2006).

Matrigel, another gel commonly used *in vitro*, is made up of components of the basement membrane that is secreted by the murine Engelbreth-Holm-Swarm (EHS) tumor. It is highly concentrated in laminin, heparin sulfate, proteoglycans and growth factors. Matrigel may offer another platform on which the interplay between cells and its microenvironment can be closely studied. Addition of Matrigel into 3D matrices make *in vitro* more closely related to *in vivo* because cells first have to degrade the basement membrane before it contacts the collagen-dense interstitial tissue. Therefore, mixtures of collagen and Matrigel can be used in testing malignant cells' invasive behavior (Griffith et al., 2006). Even though Matrigel resembles the basement membrane in some properties, it differs from basement membranes *in vivo* because it is less crosslinked and more susceptible to proteolysis, remodeling, and turnover, and it contains many more growth factors (Evan-Ram et al., 2006).

Established in vitro models to study cancer cell invasion

To study the invasive capabilities of cells, there have been a number of established 3D invasion assays that are commonly used, which have a higher chance to succeed in *in vivo* experiments because of their relevance to the physiological environment. The Transwell invasion assay is based on the Boyden chamber assay. This consists of two medium-containing chambers that are separated by a porous membrane that is coated with a thin layer of ECM on the side bordering the top chamber, on which the cells are seeded. The ECM blocks the membrane pores and allows invasive cells to degrade the matrix, invade through the thin layer, and migrate to the bottom of the filter. Subsequently, the invasive cells are quantified through staining or cell counting through

light microscopy. Advantages of using this assay are that there are many different types of cell culture inserts available and the experiment is relatively easy to set up. However, if cell staining is used to quantify the results, cells that did not invade and remained on the top of the Transwell insert need to be removed before staining the cells that were able to invade. This is done by using cotton swabs and is generally difficult, non-quantitative, and not always successful. Variations in the thickness of the ECM coating the top of the membrane and nonhomogeneous cell distribution can also present problems (Felder et al., 2013) (Zimmerman et al., 2013).

The Circular Invasion assay (CIA) is an adaptation of the common 2D wound assay (Kam et al., 2008). Instead of using sharp objects that may damage the cells and the ECM, Yu et al. used a specialized self-stick silicone cell stopper to prevent cells from growing in an allotted space. After cells had adhered to the dish, the stopper is removed and Matrigel is cast above the cells and allowed to solidify (Yu et al., 2012). To observe the invasive behavior of the cells, cells can be imaged in time lapse using fluoresced probes for proteins or cells can be fixed and stains to image after allotted invasion time. Yu et al. has observed that in this system, high resolution images are easier to obtain in the CIA over most 3D embedded experiments because staining often produces weak signals in 3D platforms and additionally, it is difficult to image through thick gels. However, this assay is much lower throughput than the Transwell chamber assay (Kam et al, 2008).

A vertical gel 3D assay can be used to study migration and invasion, in which cancerous cells are seeded on top of collagen gels that are a few millimeters thick. The vertical 3D migration, or invasion into the collagen gel, is monitored using optical

sectioning and counting the cells or using radioactive labeled cells and scintillation counting. Skin cancer is mimicked by this assay and makes it a physiologically relevant system to study invasion. However, technical difficulties arise with the recapitulation of the 3D environment. Determining whether the cells plated on top of the collagen gel invaded downwards into the gel is difficult using normal bright field microscopy because there is no clear border at the interface between the seeded cells and the top boundary of the gel. An alternative method to quantify the invasion of the cells is immunohistochemical staining followed by image analysis software, which is time-consuming and low-throughput. (Kramer et al., 2013).

Recently, Brekhman et al. used a 3D invasion assay where the cells are seeded in between two gel layers. From the start of the experiment, the cells are completely embedded in the ECM. The two gels below and above the tumor cell can have different tunable properties by varying the composition of the ECM that the cells contact. Therefore, this asymmetric assay can reveal how each gel affects the cell behavior and compare their attractive or repulsive effects upon invasion, and can also compare two different microenvironments in one single assay. Another advantage is that there is a defined origin between the two gels where invasion begins, so that the invasion can be easily quantified. Moreover, the whole cell population can be monitored which is important for the characterization of subpopulations of tumor cells. However, compared to the Boyden chamber assay, this invasion assay is relatively slow and requires more expensive and complicated equipment since it requires sectioning in a cryostat (Pouliout et al, 2013).

Tumor cells cluster together *in vivo* and can be represented as suspended multicellular spheroids *in vitro*, which mimics *in vivo* systems because tumor cells invade the surrounding tissue originating from cancer cell clusters, which have resembling cell-cell interactions (Kramer et al., 2013). The spheroid invasion model allows cells to reside in a 3D structure with cell-cell interactions that reflect *in vivo* behaviors and studies the invasive property of a certain cell type (cell type A) into another cell type that is typically a tissue like structure (cell type B). In this experiment, spheroids of cell type B are co-cultivated with cell type A, which attaches to the spheroid surface and slowly invades the spheroid. Fluorescently labeled cells allow analysis of 3D migration or invasion by confocal fluorescence microscopy. Flow cytometry must be done to differentiate between cells attached to the surface of the spheroid from cells that had truly invaded. A different route is to fix the cells and either use immunofluorescence or immunohistochemistry to analyze the results. (Zimmerman et al., 2013). Unfortunately, the entire assay itself and quantification of the invading cells are both time consuming and requires deep confocal imaging or sample preparation for immunohistochemistry and tissue sectioning equipment (Kramer et al., 2013) (Brekhman 2009).

Bioengineering has embraced 3D systems and designed multiple platforms that can be used in these studies. Microfluidic devices allow cells to be placed in specific positions and patterns within a 3D matrix, which has recently shown the significant influence of matrix composition upon the invasive characteristics of mammary fibroblasts. Synthetic materials have recently been included into 3D matrices because of its reproducibility. Materials such as polyethylene glycol, poly-lactide-co-glycolide, and hyaluronan or alginate-based hydrogels have been introduced into 3D culture systems.

The clear advantages of these biomaterials is that reproducibility can be ensured, properties such as stiffness can be carefully controlled, and biological characteristics such as integrin binding domains can be introduced (Zimmerman et al., 2013) (Pouliot et al., 2013).

Although there are advantages of 3D system compared to 2D systems, this relatively new platform has room to improve. As stated in the assays above, it is challenging for 3D methodologies to be high throughput. In addition, these experiments consume more time, and require expensive and highly technical imaging technology for data analysis (Eccles et al., 2013). 3D platforms are also generally more expensive and all the materials become a toll to the average research laboratory (Pouliot et al., 2013). Incorporating the experimental ease of 2D systems into the physiologically relevant 3D platforms could help eliminate some of the technical issues that have been plaguing this recent rise in cancer metastasis research.

Novel "2.5D" assay designed to study cancer invasion at high magnification

We have utilized a platform in which we have combined the simplicity of 2D assays with the physiological relevance of the 3D environment, which reflects a truly novel "2.5D" system. Traditional cancer biology has followed the principle of durotaxis, when cell migration moves up the rigidity gradient (Wang et al., 2000). With this 2.5D system, we have uncovered that this migration mode is not always the case, which in itself is an unexpected phenomenon. Cells have the ability to invade from a rigid substrate into a softer 3D matrix cast above it. A clinical example of this in vitro assay is osteosarcoma, the most common primary bone cancer that occurs in children and young

adolescents (Daw et al., 2005). Osteosarcoma travels with highest frequency to the lung, and for metastasis to take place, the bone cancer cells need to invade into surrounding tissues which are softer than the bone. This process is mimicked by our system in terms of the direction that the cells move in the rigidity gradient (Hayden et al., 2005) (Clark et al., 2007).

A novel aspect of this assay is the capability of studying the transition of cell morphology at high-resolution, in particular the effects upon the cytoskeleton of casting a 3D matrix above a monolayer of cells. High resolution is possible because the cells are near the bottom of the 2D substrate, which allows close contact between the lens and the object. Through 12-hour live cell imaging right after the cells were in contact with the gel, we captured cells transiting from 2D morphology to 3D morphology, showing that the cells adapted to the 3D environment. Additionally, this assay enabled us to accurately quantify the fraction of cells that invaded into the matrix and the height to which they can travel above the 2D interface, which has been a consistent challenge for other 3D assays. This "2.5D" assay is an ideal platform to study cancer cell invasion because it offers a methodology to capture cells in high magnification as well as their journey into the 3D matrix.

Using the first function of this assay, we discovered long, thin, actin-dense spikes lining the cell membrane that may play a role in cancer cell invasion. Through investigating how cells invade, we determined that varying the mechanical properties of the substrate beneath the cells and the concentration of matrix above them do not change the fraction of cells that invade into the gel. Integrating shRNA technique and drug inhibitions, we showed that these spikes were most likely not filopodia. Even though the

identity of the microspikes still remains unknown, results suggest that the microspikes are required but not sufficient for invasion. Further examination of the properties of these protrusions showed that cells still retain a significant amount of their ability to invade the gel without the functions of actomyosin proteins, cell-ECM interaction, and degradation of the ECM. Through examining a wide variety of cell lines, ranging from breast, pancreatic cancer, and fibrosarcoma cells to noncancerous cells, we established a correlation between whether the cells were able to form the spikes and whether invasion was a possibility. This can be a quick detection of whether a certain cell line is invasive without conducting long-term assays and time consuming quantification procedures.

Experimental Procedures

Cell culture

Human breast carcinoma cells MDA-MB-231(Physical Sciences Oncology Center, NIH), human fibrosarcoma HT1080 (ATCC) and mouse embryonic fibroblast MEF (ATCC) cells were cultured in Dulbecco's modified Eagle's medium (Mediatech Inc.), high glucose (4.5 g/L), supplemented with 10% fetal bovine serum (Hyclone) and 1 % Pen/Strep (Sigma). PAC001, PAC008, and PAC009 (Maitra Lab, Johns Hopkins Pathology) were cultured in Dulbecco's modified Eagle's medium (Gibco), high glucose (4.5 g/L), no sodium pyruvate, supplemented with 10% fetal bovine serum (Benchmark) and 1% Pen/Strep (Sigma). PAC011 cells cultured in M3 base culture media (Incell Corporation), Dulbecco's modified Eagle's medium (Gibco), low glucose (1 g/L), and supplemented with 5% fetal bovine serum (Benchmark FBS), 25μg/ml gentamycin (Ameresco), 10 ng/ml EGF (Cell Signaling Technologies), and 1% Pen/Strep (Sigma). U2OS cells (ATCC) were cultured in McCoy's 5a Medium Modified (Gibco) supplemented with 10% fetal bovine serum (Hyclone) and 1 % Pen/Strep (Sigma) All the cells were maintained in an incubator with 5% CO_2 at 37 °C.

2D collagen I-coated substrates

Two-dimensional cell-culture glass-bottom 24-well plates (BD Biosciences) were coated with soluble rat tail type I collagen in acetic acid (BD Biosciences) to achieve a coverage of 60 μg/cm^2 and incubated at room temperature for 2 h. This concentration was chosen to saturate the surface of the wells. Plates were then washed gently three times with PBS and seeded with cells.

2.5D collagen I matrices

Wells seed with cells were washed gently with PBS. 2.5D collagen matrices were prepared with soluble rat tail type I collagen in acetic acid (BD Biosciences) to achieve a final concentrations of 1, 2, and 4 mg/ml collagen. 1 M NaOH was then added to normalize pH to about 7.0. Remaining volume filled with a 1:1 ratio of reconstitution buffer and culture medium. The mixture was placed in 24-well culture plates (BD Biosciences). Collagen gels solidified within 1h in an incubator at 37°C and 5% CO_2, then 500 µl of cell culture medium was added.

Immunofluorescence microscopy

Immunofluorescence in 3D was performed as described previously (Giri et al., 2013). Briefly, cells were plated under collagen gels as mentioned above (2.5D collagen I matrices). After 2 h, cells were fixed with 4% formaldehyde for 30 min and permeabilized with extraction buffer consisting of 0.1% Triton-X 100 (v/v) for 30 min. Cells were then incubated overnight at 4°C with phalloidin (Abcam, Cambridge, MA, USA) at a 1:20 dilution ratio, and washed 3 times with PBS for 30 min each. Cells at 2.5D were then imaged using a Nikon A1 confocal microscope using a ×60 water-immersion lens.

Stable expression of Life-act-EGFP and H2B-mCherry

The plasmid encoding H2B-mCherry in a lentiviral vector with phosphoglycerate kinase promoter (PGK) was obtained from Addgene (Plasmid 21217). The plasmid encoding Lifeact-EGFP in a lentiviral vector was constructed as previously described (Lee et al.,

2012; Riedl et al., 2008). To generate lentivirus particles, HEK293T cells were co-transfected with three plasmids (lentiviral vector, ΔR 8.91, and pMDG-VSVG) using Fugene HD (Promega). The medium was replaced with fresh medium 24 h after transfection. The lentiviral particles were harvested another 24 h later immediately filtered through 0.45-μm filter (Millipore) to remove cellular debris, and then stored at −80°C. For transduction, 1×10^5 cells in a 35-mm culture dish were transduced with lentivirus. Stable expression of Lifeact-EGFP and H2B-mCherry was validated two or three days after transduction using a Nikon TE2000E epifluorescence microscope (Nikon).

Depletion of integrin by shRNAs

The RNAi sequences targeting mRNA of β1 integrin were selected using the RNAi design online program from Dharmacon (http://www.dharmacon.com). Two targeting sites were chosen. The sequences used were TGCCTACTTCTGCACGATGT (174) and CCAGCCCATTTAGCTACAAA (674). Successful depletion of the protein was confirmed by Western blotting and quantified using ImageJ (NIH).

Fraction of Cells that Invaded in to the Gel

Images of cells were collected during live cell imaging using a Cascade 1K CCD camera (Roper Scientific) mounted on a Nikon TE2000E phase contrast microscope equipped with a 10x objective (Nikon) and controlled by NIS-Elements AR imaging software (Nikon). Z-stacks in 5.0 μm intervals were used to image the cells from the 2.5D interface to the highest cell visualized in the cell.

Quantifying Fraction of Cells in the Gel

NIS-Elements-AR was used to analyze the cells in the gel starting from the lowest z-position of the gel at the 2.5D interface with the cells in focused. All the cells, including the cells at the edges, in this frame were counted and these cells were labeled as cells still at the 2.5D interface. Cells 15-20μm above this 2.5D interface were counted as cells in the gel, to ensure that the cells had fully invaded into the gel. The number of cells which migrated into the gel and remained at the bottom were counted as N_{gel} and N_{bottom}. The fraction of cells in the gel was calculated as N_{gel} /(N_{gel} + N_{bottom}).

Quantifying Number of Microspikes Per Cell

NIS-Elements-AR was used to determine the number of spikes per cell, by imaging the entire thickness of the cell through z-stacks. Maximum intensity projection was used to make sure every dimension of the cell was captured. Any protrusion was counted as a microspike if the spike originated from the cell body and was very thin. Spikes that sprouted from another spike were not counted as an individual spike. Length was not a factor in this quantification.

Drugs inhibition experiments

Drugs for inhibition were added to the media when the cells were seeded and also once again when the gel was cast. During both additions, concentrations for each respective drug were the same. Drugs used in this work were 10 μM of Marimastat Inhibitor

(AnSpec Inc.), 10 μM Blebbistatin (Sigma), 1 μg/ml Nocodazle (Sigma), and 250nM Latrunculin B (Sigma).

Statistical analysis

All the experiments were repeated at least three times (three distinct biological repeats) for statistical analysis. The mean ± standard error (SE) was determined and statistical analysis was performed with the use of Graphpad Prism (Graphpad Software). Two-tailed unpaired *t*-tests and one-way analysis of variance were conducted to determine the significance of samples with two groups and more than two groups, as indicated by the standard Michelin Guide scale ($^{***}p < 0.001$, $^{**}p < 0.01$, and $^{*}p < 0.05$). Linear regressions were calculated and plotted using Graphpad Prism for correlation plots. Slope and square of the Pearson correlation coefficient (R^2) of the regression's deviation from zero slope are shown in the plots.

Acknowledgements

We thank Anjil Giri (Johns Hopkins University, USA) for providing us with fascin, cdc42, and myosin X knockdown HT1080 cells. We thank Jude Philip (Johns Hopkins University, USA) for providing us with PAC001, PAC008, PAC009, and PAC01 cells.

RESULTS

Cells morphologically transit and invade from a rigid 2D substrate to a softer 3D matrix

Traditionally, cells have an increased likelihood to move towards substrates of increased stiffness, a phenomenon known as durotaxis (Lo et al., 2000). In previous work, fibroblasts were observed to preferentially move towards substrates with a stiffer rigidity and retract their leading edge when they reached the boundary between the stiffer substrate and a softer material (Wang et al. 2000). In our work, we tested this widely accepted principle by investigating whether cells would invade from a rigid substrate to a soft matrix. We first plated cells upon collagen coated plates and then cast 3D matrices above the adhered cells 24 hours later, establishing a "2.5D" system, and observed changes over time. We employed a 3D matrix composed of Type I collagen, the primary component of the ECM, and the home of HT1080 fibrosarcoma cells.

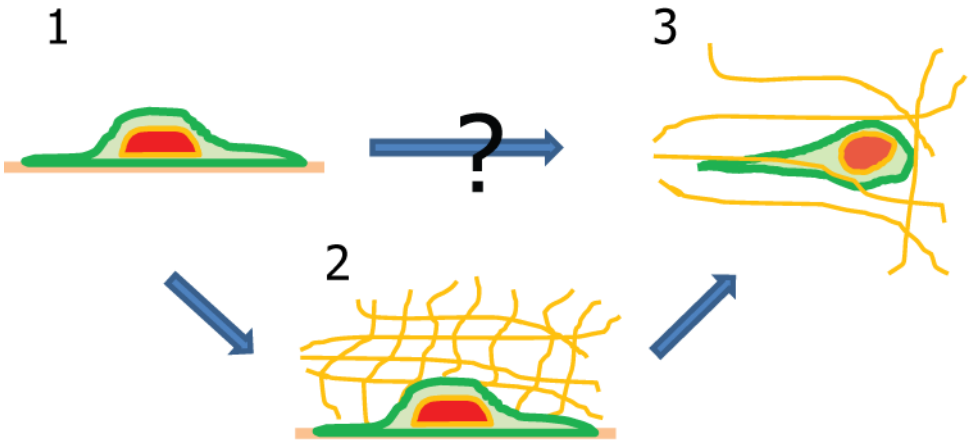

Figure 5: Cell transitioning from 2D to 3D. **(1)** Cell adhered to collagen coated substrate. **(2)** Collagen gel cast above cells. **(3)** Cell transformed to 3D morphology. Our work

focused on whether the casting of a collagen matrix would cause the morphological transition of cells originally of 2D morphology (1) to shift to 3D morphology (3).

Using Collagen Type I- FITC Conjugate, we managed to visualize the collagen gel with confocal microscopy and observed the localization of the cells in the collagen gel (See Figure 6A and 6B). This experiment provided a direct visual of the 2.5D system, in which majority of cells still adhered to the glass substrate and a small percentage of cells that detached and subsequently invaded into the matrix. The fluorescence of the collagen and the cells provide a broad overview of the cells position in the 2.5D system. The defined, clear focal plane of the 2.5D interface makes it easy to identify the cells that detached from the substrate. Furthermore, we captured a cell in the process of detaching and found that the part of the cell still adhered to the substrate does not show assembly of microspikes, while the other half of the cell climbing into the gel shows microspike formation (See Figure 6C). This observation triggered our interest in further investigating the morphological transition of cells from 2D to 3D at the 2.5 interface.

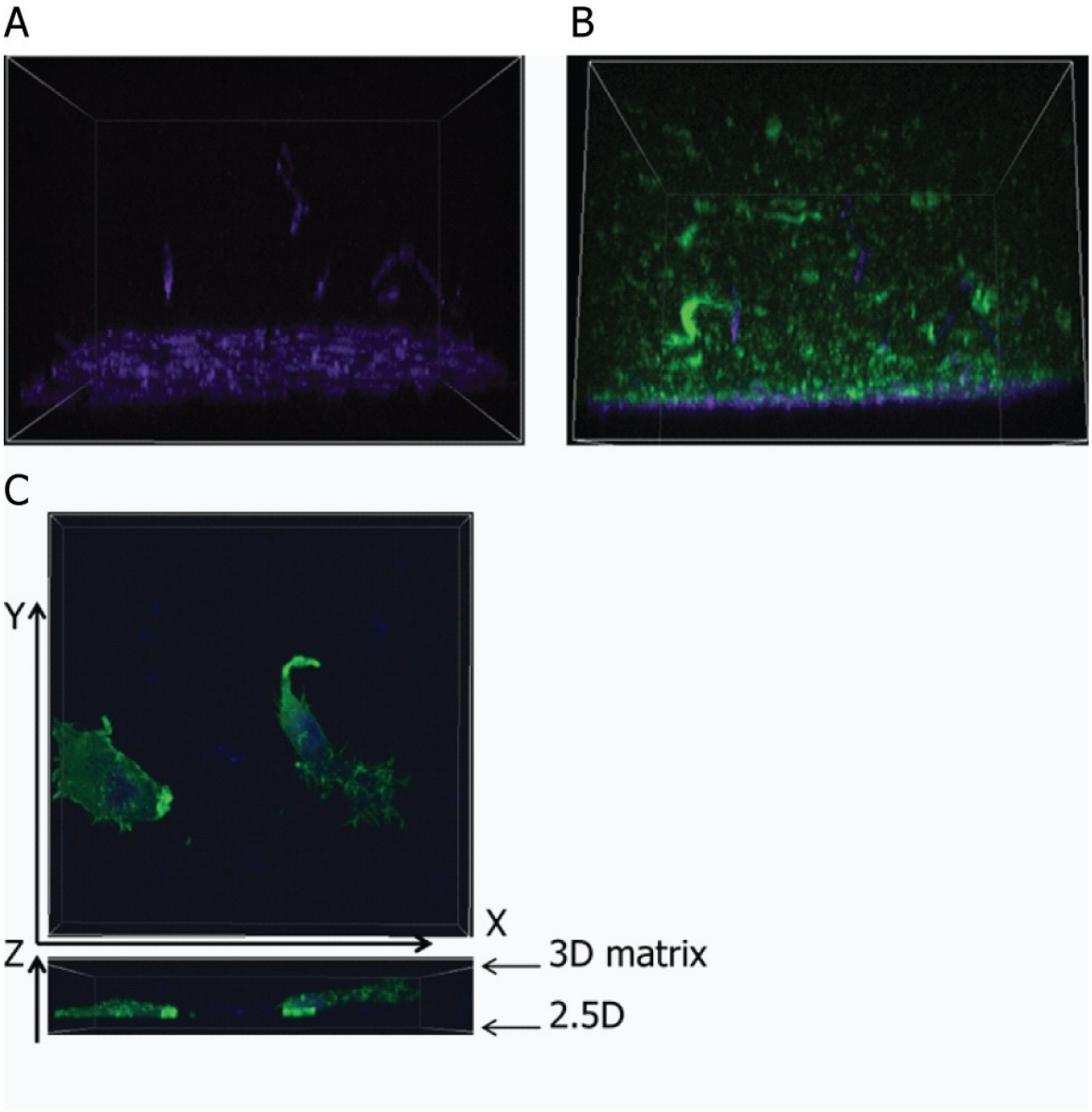

Figure 6: Invasion of cells from 2D substrate to 3D collagen matrix revealed by fluorescently stained or labeled cells and collagen**. (A)** Cells were stained with Phalloidin-643 and shown in purple here. **(B)** Collagen Type I-FITC is shown in green. The majority of the cells are at the 2D interface and a low fraction of cells are dispersed throughout the collagen gel. **(C) A** cell captured in the process of detaching from the 2D substrate and invading into the 3D collagen.

Cells adhered to a 2D substrate and immersed in a 3D gel display many different morphological characteristics. Previous research shows that human fibroblasts on 2D collagen substrates were broader, more flattened, and displayed more lamellae than their counterparts in 3D collagen matrices. Cells embedded in 3D collagen matrices show a more elongated morphology with small or fewer lamaelle and are also substantially less spread than on a 2D substrate (Hakkinen et al., 2011). To verify that cells in our system presented similar transformations, we put HT1080 fibrosarcoma cells in a 2D, 2.5D, and 3D systems to compare phenotypic differences. We used high-resolution confocal microscopy to image HT1080 stably expressing H2B-mCherry to assess the morphology of the cells. As expected, HT1080 cells adhered to a 2D substrate displayed broad lamellipodia and were more spread upon the substrate (See Figure 7A). After cells were in contact with the collagen gel for two hours, we discovered that the cells immediately responded to the collagen gel stimuli and already began the physical transformation. They assembled thin microspikes that lined the cell body but still displayed broad lamellipodia (See Figure 7B). Cells embedded in a 3D collagen gel formed long spikey protrusions and had an overall elongated cell morphology (See Figure 7C). As predicted, these cells were much less spread than cells in the other two systems described.

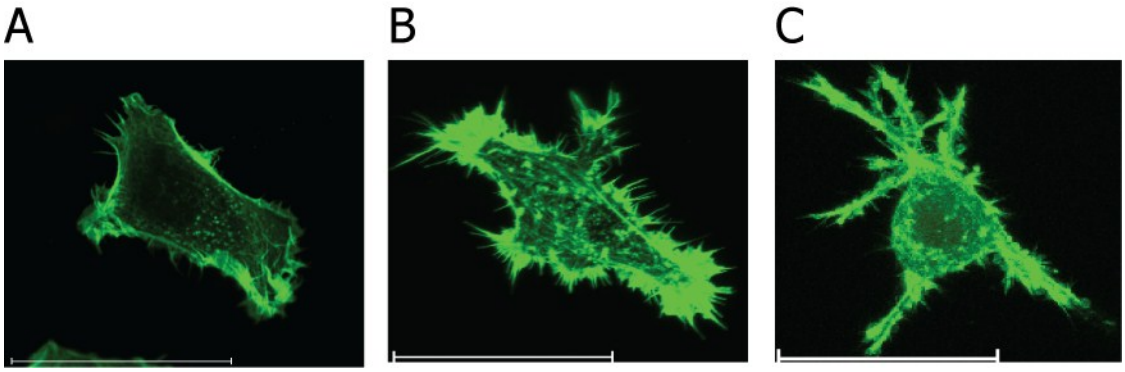

Figure 7: HT1080 cells in 2D, 2.5D, and 3D systems are stained with phalloidin-488. Images were taken using CLSM with a 60X water lens. (A) A spread HT1080 cell adhered on a collagen-coated substrate. In a 2D system, the cell does not exhibit microspikes. (B) F-actin staining in HT1080 cell two hours after collagen gel casting. The instantaneous response to the collagen gel is captured here, with upwards of 50 spikes per cell. (C) HT1080 cell two hours after embedded into a collagen gel. The elongated protrusions are characteristic of 3D cells and are different from the microspikes on the cells at the 2.5D interface.

To obtain a clearer understanding of this phenomenon, we monitored the physical transition of cells from 2D to 3D over a twelve-hour span using live cell confocal microscopy. The overall transition from 2D to 3D morphology remarkably exhibits the effects of the collagen matrix upon the cells. Through our 2.5D assay, we were able to obtain images of the cells in high magnification because of the distinct interface between the substrate and the gel. To study the changes in morphology of the nucleus and actin cytoskeleton, we used HT1080 cells stably expressing Life-act-EGFP and H2B-mCherry. Just after two hours, cells already displayed drastic changes. Formation of actin-rich

"microspikes" lined the cell membrane, with spikes extending from broad lamellipodia characteristic of 2D cell morphology (See Figure 8). Around six hours after the initial gel casting, the cytoskeleton began to rearrange from broad lamellipodia common of 2D cell morphology into thinner protrusions that are a distinctive property of 3D cells. At 12 hours, the cells exhibited 3D-type morphology still displaying the microspikes. Because the microspikes were present during the entire transformation, we hypothesized that they may potentially play a role in cancer invasion.

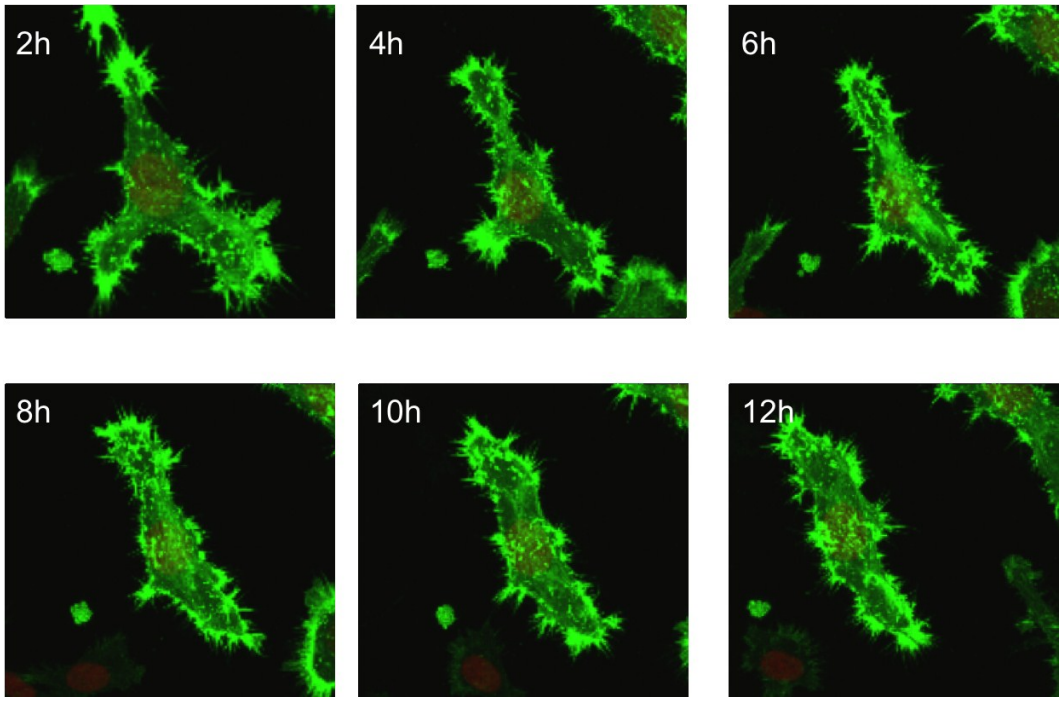

Figure 8: The morphological transition of HT1080 in response to collagen gel stimuli**.** HT1080 cells stably expressing Life-act-EGFP and H2B-mCherry were imaged using live cell confocal microscopy over a span of 12 hours. The cell depicted is morphologically transitioning from 2D to 3D. At two hours, cells already formed microspikes and at 8 hours, the cell shifted towards a 3D phenotype and became more elongated and protruded. `

Cells invade based upon superdiffusion over time and invasion is highly dependent on cell density

To analyze trends over a longer period of time, we monitored the invasion process of cells in the 2.5D system ranging from two to six days. 2mg/ml collagen gels were cast above the cells seeded on collagen coated wells and then incubated at 37°C for the respective amount of days. Both the fraction of cells in the gel and the maximum height that the cells traveled in the gel increased as time progressed (See Figure 9A). In comparison to two days after gelation, the increase of fraction invaded into the gel for three, four, and six days are all significant (* = $p < 0.05$, * = $p < 0.05$, and *** = $p < 0.001$ respectively). We took proliferation into account by analyzing the proliferation rates of cells at the interface and cells that invaded into the gel. The proliferation rates of the cells at the interface were higher than that of the cells in the gel. In addition, cells traveled higher distances into the gel as time progressed, showing that cells continued to degrade their way through intact collagen meshes (See Figure 9B). In comparison to distances two days after gelation, the highest distances that the cells traveled into the gel three, four, and six days after gelation are all significant ($^{***}p < 0.001$ for all three). Using a diffusion-based model, we determined that the cells are not invading the gel through simple diffusion, and that there is a driving force causing the cells to invade (See Figure 9C). These results suggest that the appearance of cells in the 3D matrix did not result solely from diffusion but involves active contribution from the cells.

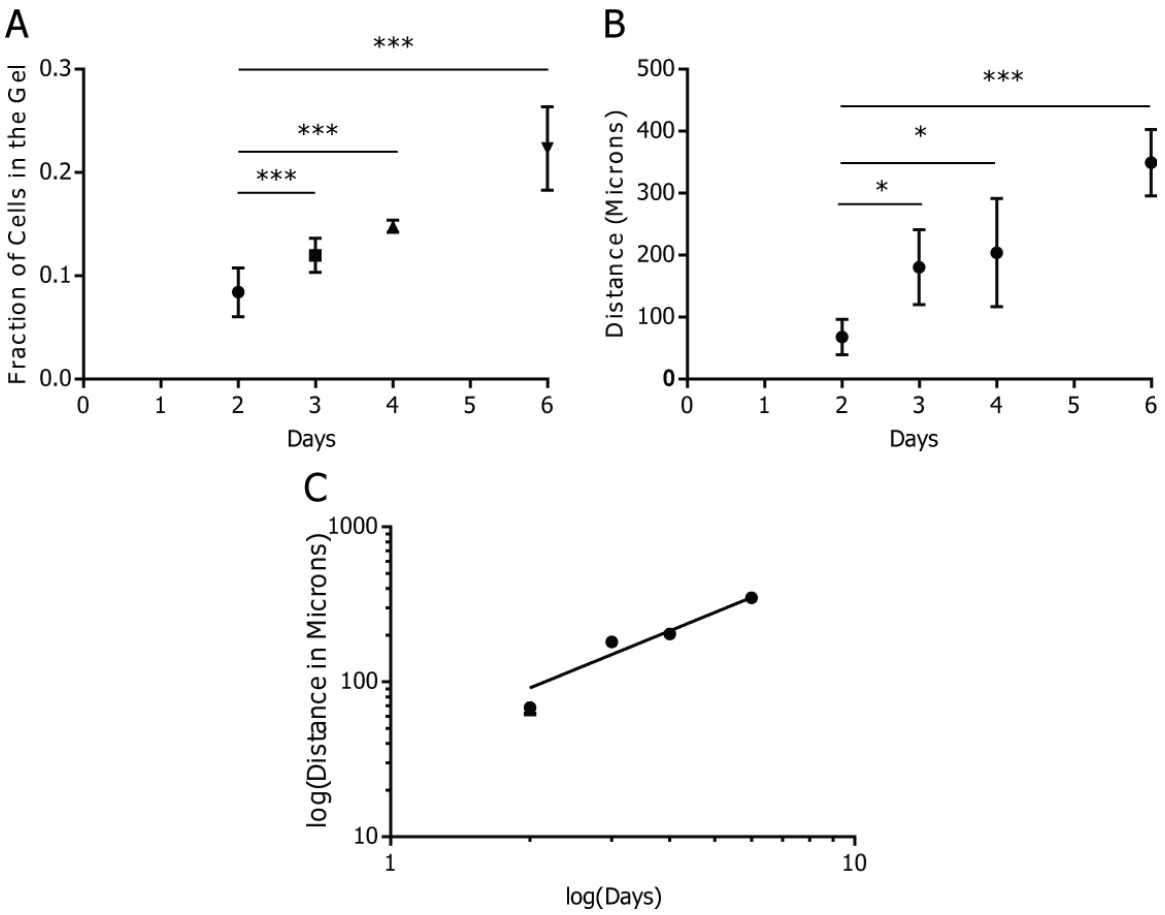

Figure 9: The fraction of cells invading into the 3D matrix and the highest distance that cells travel into the matrix over time. **(A)** Fraction of HT1080 cells that invaded into the gel ranging from 2 days to 6 days, showing an increase in the fraction of cells that invaded over time. **(B)** Highest distance that HT1080 cells travelled in the gel measured over the same time span. As days progressed, cells were able to climb to higher heights **(C)** Trendline of the transformed diffusion graph is log(Distance in Microns) = 1.223 log(time) + 39.19 of the power law: distance = $39.19*time^{1.223}$. The slope of 1.223 is the dependence of distance on time. This signifies that invasion is not solely simple diffusion, where the dependence would be a value of 0.5 ($time^{0.5}$ α distance), and that there is an active driving force in this phenomenon.

Our results show that cell density plays an extremely important role in both the fraction of cells that invade and the highest distance traveled in the gel. We plated HT1080 cells at 1.25K/well, 2.5K/well, and 5K/well. The doubling of cell density results in a linear trend of cells invading from the 2D substrate (See Figure 10A). However, a two-fold increase in cell density produces exponential increases in the highest distance traveled in the gel, suggesting that there is an active force behind this phenomenon (See Figure 10B).

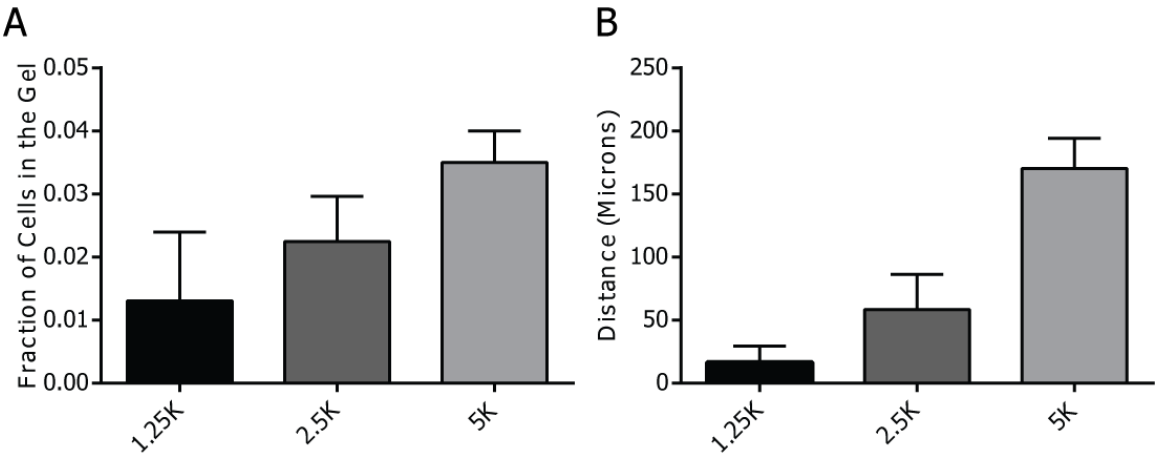

Figure 10: The dependence of cell invasion on cell density. All samples were analyzed three days after the gelation of the collagen matrix. **(A)** Fraction of cells that invaded for different cell densities appears to increase in a linear trend. **(B)** Highest distance that the cells travelled in the gel increases as the density of cells at the 2.5D interface increases. Dependence of highest distance in the gel on cell density increases in an exponential manner, suggesting that there are additional driving forces involved.

Altering the external properties of the microenvironment does not affect HT1080 invasion

The density of the matrix affects how easily the cells can migrate and invade through the gel based on previous investigation into single HT1080 cell migration in 3D matrices (Unpublished work from Wirtz Lab). To study how the behavior of cells varies with changing matrix properties, different concentrations of collagen gels were made, ranging from 1 mg/ml to 4 mg/ml. Interestingly, the differences in collagen concentration did not change the fraction of HT1080 cells that invaded into the gel three days after gelation (See Figure 11A). Another parameter tested was the rigidity of the substrate beneath the cells. Using polyacrylamide gels, the Young's modulus of the collagen coated glass (500kPa) was altered to either the "stiff" PAA gel (5kPa) or soft PAA (< 1 kPa). After 3 days of incubation, HT1080 cells showed approximately the same fraction of cells invaded into the gel as with the glass control. These results suggest that the stiffness of the substrate beneath the cells do not have any affect upon the likelihood of HT1080 cells to invade in this 2.5D system (See Figure 11B).

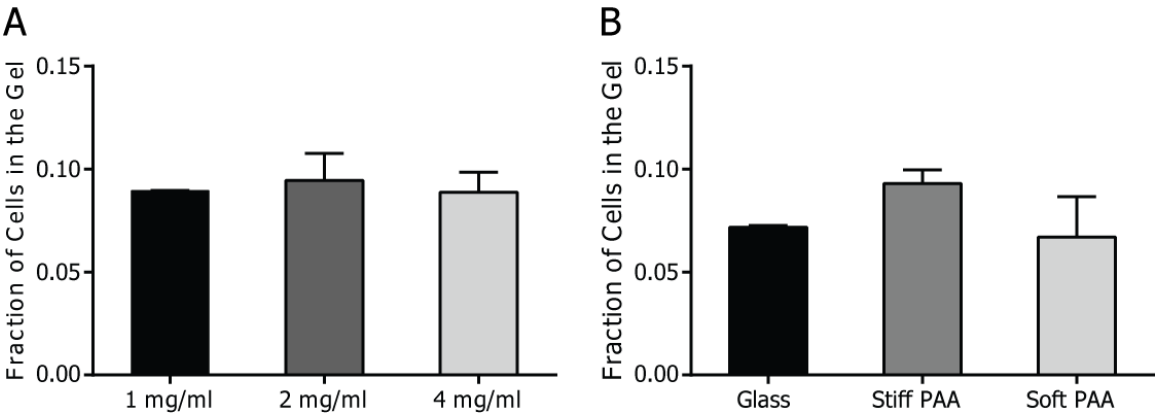

Figure 11: The effects of varying external properties of the 2.5D system in the invasion of HT1080 cells. **(A)** Fraction of HT1080 cells that invaded into the gel at 1mg/ml, 2mg/ml, and 4 mg/ml collagen gels after three days. The concentration of collagen gel does not affect the fraction of cells that invade. **(B)** Fraction of HT1080 cells that invaded after seeded on different rigidities of polyacrylamide gels after three days. The Young's modulus of glass, stiff PAA and soft PAA are 500kPa, 5kPa, and < 1kPa respectively. The rigidity of the substrate beneath the cell does not affect the fraction of cells that invade either.

Cells can invade at low concentrations of collagen gel independent of MMP, myosin II, and β-1 integrin

Based on the finding that there is an active force driving cells to invade, we explored potential mechanisms that control cell invasion. To investigate what controls invasion, cells were treated with drugs inhibiting MMPs, myosin II, actin, and microtubules, and shRNA knockdown of integrin, which are all involved in cell migration (Sahai et al., 2005). Western blots confirmed that the lentivirus transfections of β-1 integrin were successful (See Figure 12). To observe the morphological

differences between the cells treated with drugs and shRNA knockdown, cells were fixed and stained two hours after gelation of a 2 mg/ml collagen gel (See Figure 13). Along with our standard 2 mg/ml collagen gel, we also experimented with a less dense gel of 1 mg/ml and a more stiff gel of 4 mg/ml. In 1 mg/ml, cells were still able to invade with the treatment of marimastat, which blocks MMP, and blebbistatin, which blocks myosin II, and with reduced expression level of β-1 integrin, which interacts with the ECM through binding onto RGD peptides (See Figure 14A). In the two higher concentrations of collagen gels, the cells lost their ability to invade with treatment of marimastat and blebbistatin as well as the depletion of integrin. Lack of the cytoskeleton assembly caused by LatB and nocodazole prohibited the cells from invading at all the tested any concentrations of collagen matrix, suggesting that the cytoskeleton is critical for any type of cell movement. (See Figure 14B and 14C).

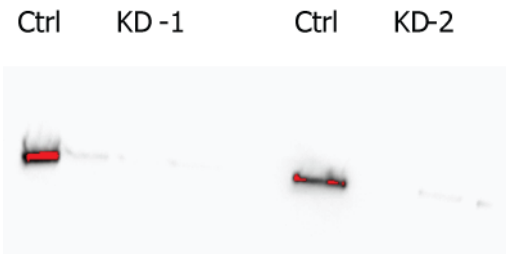

Figure 12: Western Blot of the expression of β-1 integrin in wild type and integrin depleted HT1080 cells**.** For both shRNA knockdowns, the levels of β-1 integrin are insignificant compared to the HT1080 wild type, signifying that the protein is effectively depleted from the cells.

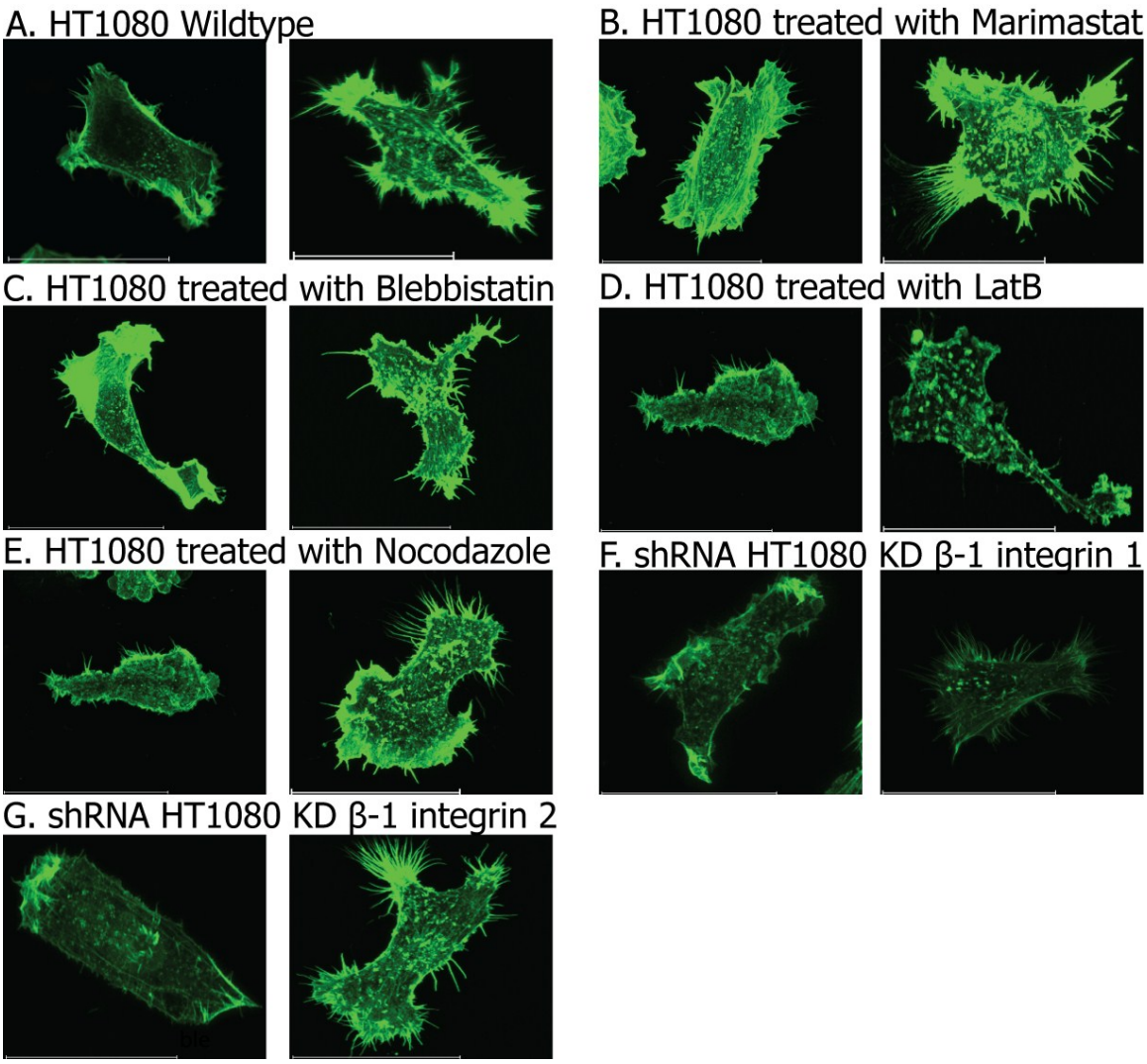

Figure 13: Images of HT1080 Cells Treated with Drugs and shRNA knockdowns. HT1080 cells in 2D adhered to a collagen coated substrate (left) and HT1080 cells in a 2.5D system two hours after gelation (right) were stained for actin with Phalloidin-488 and shown in green. (A) HT1080 wild type cells. (B) HT1080 cells treated with marimastat. (C) HT1080 cells treated with blebbistatin. (D) HT1080 cells treated with latrunculin B. (E) HT1080 cells treated with nocodazole. (F) First shRNA HT1080 knockdown of β-1 integrin. (G) Second shRNA HT1080 knockdown of β-1 integrin.

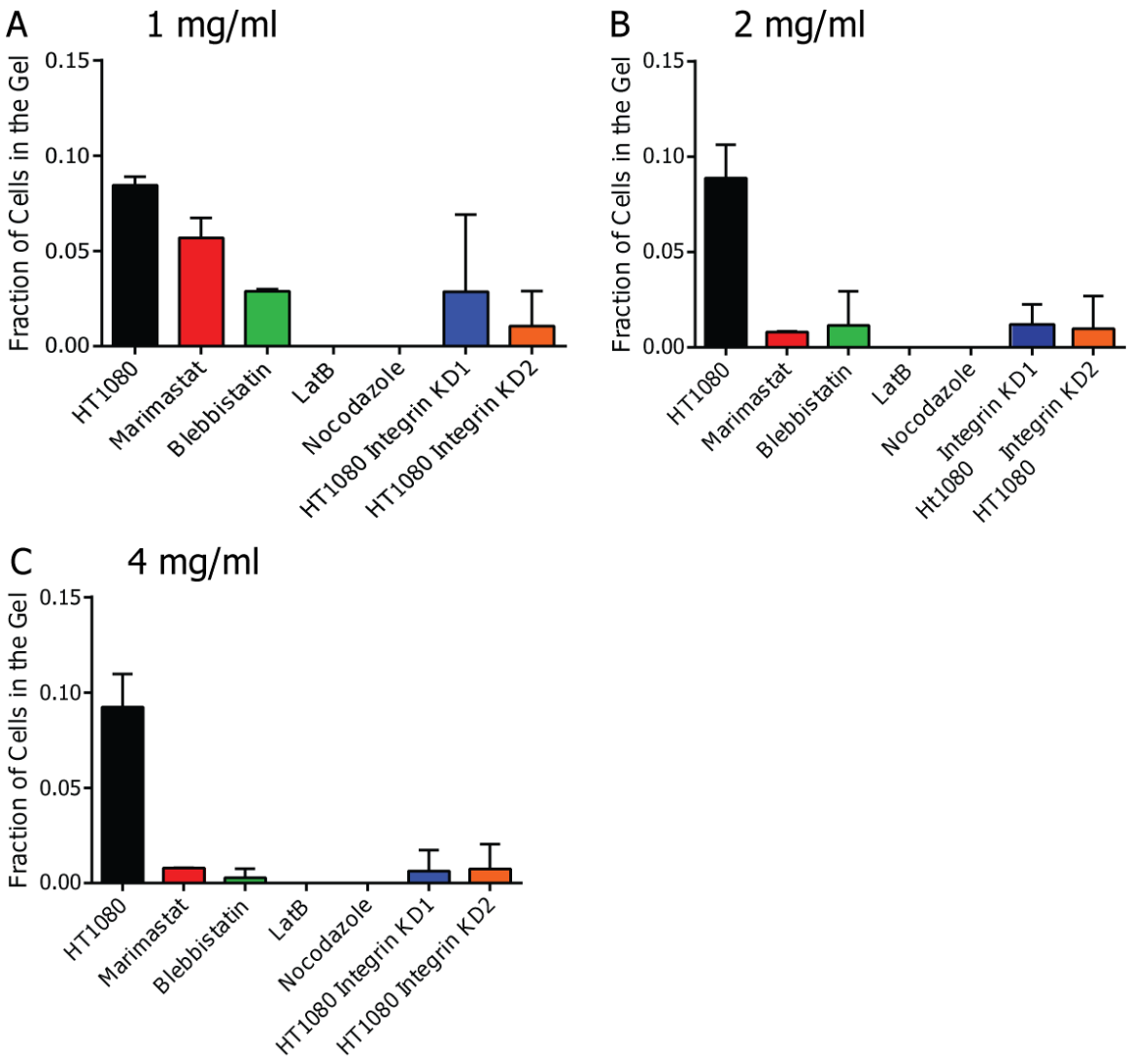

Figure 14: The effects on cell invasion by blocking or depleting cell motility-related molecules in different concentrations of collagen matrices. HT1080 cells are either depleted of β-1 integrin or treated with marimastat, blebbistatin, latrunculin B, or nocodazole. The fractions of cells that invaded in different concentrations of collagen are plotted. **(A)** In 1 mg/ml collagen matrix, cells can still invade with the treatment of marimastat, blebbistatin, and shRNA knockdown of β-1 integrin, showing that the cell does not completely rely on the degradation of the ECM, actomyosin proteins, and cell-ECM interaction to invade at this low concentration of collagen. However, the cell

cannot invade without the functions of the cytoskeleton. **(B and C)** In both 2 mg/ml and 4 mg/ml, cells show significantly reduced abilities to invade under all conditions compared to wild type HT1080 cells.

Microspikes are dependent on actin but they are not filopodia

Weinburg et al., had observed microspikes and characterized them as "filopodia like protrusions" (FLPs) that formed when cells were plated above a layer of 100% Matrigel and then covered with culture medium composed of 2% Matrigel (Weinburg et al., 2013). To identify if these microspikes were structures similar to FLPs, HT1080 cells were stained for actin and microtubules, since filopodia are actin-dense and devoid of microtubules. Results revealed that these microspikes were composed of actin and microtubules were not localized at these microspikes (See Figure 15A).

To further examine the microspikes' dependence on the cytoskeleton, HT1080 cells were treated with LatB and nocodazole, and then stained the cells with phalloidin and tubulin antibodies. When treated with LatB, which prevents F-actin assembly by blocking actin polymerization, the actin cytoskeleton was disrupted and microspikes failed to form (See Figure 15B). However, after treating the cells with nocodazole, a drug used to block microtubule formation, the cells still preserved the ability to form the thin protrusions (See Figure 15C). These results further confirmed that the microspike formation induced by the collagen gel is actin dependent and does not involve microtubules.

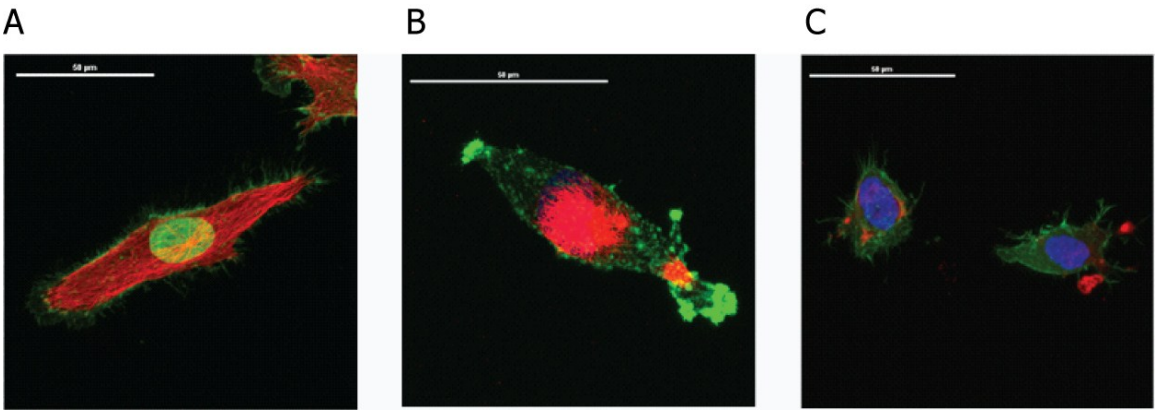

Figure 15: The dependence of microspikes on the cytoskeleton**.** Cells were plated for 24 hours and stained with phalloidin (green) and tubulin antibodies (red) 2 hours after gelation: **(A)** Wild type HT1080 cell exhibiting he microspikes, which are actin-dense without the presence of microtubules. **(B)** HT1080 treated with LatB showed that the microspikes failed to form without actin filaments assembled. **(C)** HT1080 treated with nocodozole are capapble of forming the microspikes in the absence of microtubules.

To further characterize the properties of the microspikes, potential signaling pathways involved were investigated using HT1080 knockdown cells of proteins involved in filopodia formation. Cdc42 is an upstream protein that recruits other proteins that synergistically induce filopodia formation (Ridley 2011). Myosin X is the motor protein that traffics cargo, including β-1 integrin, to the tips of filopodia where these proteins can interact with the ECM. Bohil et al. demonstrated that myosin X is a strong inducer of filopodia and can even induce filopodia without substrate adhesion (Bohil et al, 2006). Finally, fascin controls filopodia stability and is upregulated in many cancers (Arjonen et al., 2011). We explored how the depletion of the filopodia-associated

proteins would affect the formation of the microspikes by using one shRNA fascin knockdown, two shRNA cdc42 knockdowns, and two shRNA myosin X knockdowns. To ensure that the lentivirus transfection was efficient, we performed Western Blots to detect relative amounts of protein in the knockdown cells compared to HT1080 wild type cells and established that the respective proteins were truly eliminated from the cells (See Figure 16**)**. We cultured them in selective media with puromycin to ensure that only the cells infected with the virus, which encodes a gene to allow the transfected cells to be immune to puromycin, could survive.

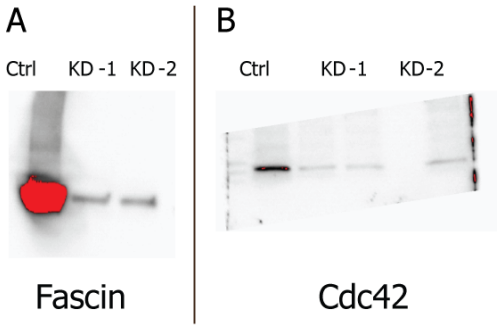

Figure 16: Western Blots to detect levels of fascin and cdc42 in respective HT1080 knockdown cells**.** Both proteins were effectively reduced in these knockdown cells compared to HT1080 wild type. (A) The levels of fascin in the shRNA HT1080 knockdown cell is significantly lower compared to HT1080 wild type. (B) For both shRNA knockdown cells, myosin X levels are significantly lower than that of the wild type cells.

We performed an identical experiment with these knockdown cell lines as with the wild type cells and allowed the cells to be in contact with the collagen gel for two

hours. Through confocal microscopy and immunostaining, we were able to obtain high-resolution images of these cells at the 2.5D interface (See Figure 17). After quantifying the number of microspikes that formed per cell of the different knockdown cell lines, results suggest that microspike formation did not depend on any of the filopodia related molecules. All of the shRNA knockdown cells were all able to form microspikes at similar quantities as their wild type form (See Figure 18A). After these experiments, we concluded that the microspikes were most likely not filopodia.

Subsequently, we tested the knockdown cell lines to examine whether the filopodia-related proteins played a role in invasion. In comparison to the baseline invasion fraction of HT1080 wild type, the majority of the knockdown cells did not display a decreased invasion percentage. The fascin knockdown and the myosin X knockdowns had approximately the same fraction of invading cells as the control HT1080 wild type, while one of the cdc42 knockdowns appeared to have an even higher fraction than the wild type (See Figure 18B)

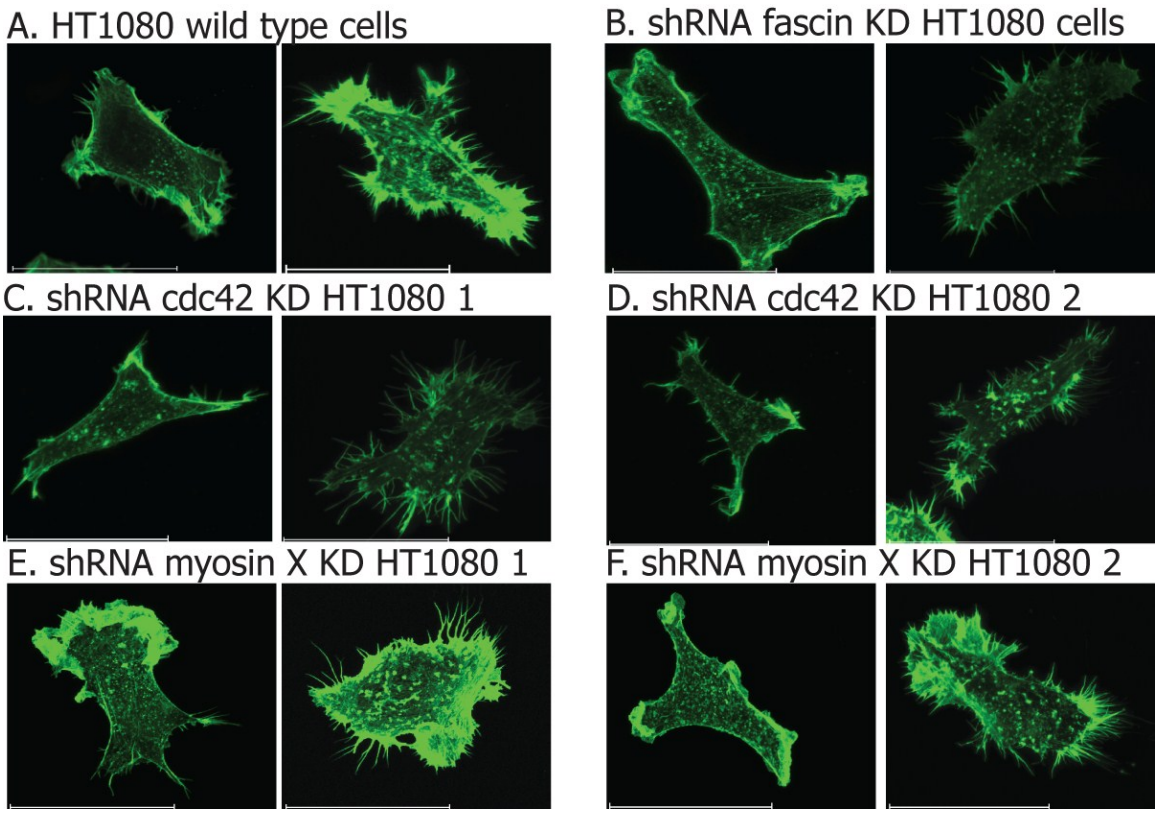

Figure 17: Filopodia-related shRNA HT1080 knockdown cells. HT1080 cells in 2D adhered to a collagen coated substrate (left) and HT1080 cells in a 2.5D system two hours after gelation (right) were fixed and stained for actin using Phalloidin-488. 2D cells do not exhibit microspikes while cells in 2.5D form more than 35 spikes per cell. **(A)** HT1080 WT cells. **(B)** shRNA HT1080 fascin knockdown cells. **(C)** First shRNA HT1080 cdc42 knockdown cells. **(D)** Second shRNA HT1080 cdc42 knockdown cells. **(E)** First shRNA HT1080 myosin X knockdown cells. **(F)** Second shRNA HT1080 myosin X knockdown cells.

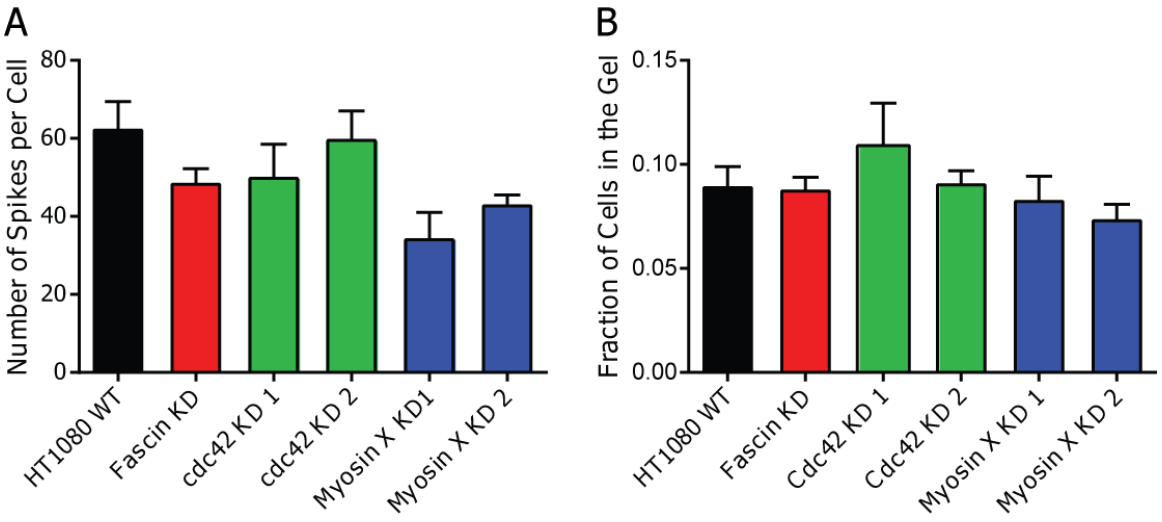

Figure 18: The depletion of filopodia-related proteins do not affect the assembly of microspikes or invasion of HT1080, suggesting that these microspike-like protrusions are most likely not filopodia. **(A)** Numbers of microspikes per cell that formed for all HT1080 knockdown cell lines. The numbers of microspikes that form per cell are not significantly different compared to HT1080 wild type. **(B)** Fractions of HT1080 knockdown cells that invaded into the gel over a three day span, which are not significant in comparison to HT1080 wild type.

Microspike formation and invasion are correlated across different cell types

In order to determine if the microspikes had any functions in invasion, we tested multiple cell lines to study if there was any correlation between the formation of the spikes and cell invasion. Our initial results focused upon HT1080 cells, which are known to be highly invasive cells. To further explore this phenomenon, we used three other well-known cell lines, the breast cancer cell line MDA-MB-231, noncancerous mouse embryonic fibroblasts, MEF, and the osteosarcoma cell line U2OS. PAC cell lines were

also included, a pancreatic cancer cell line derived from patients obtained from the Maitra Lab. PAC001 is a cell line from liver metastasis, PAC008 and PAC009 are two cell lines that are from the primary pancreatic tumor, and PAC011 cells originated from normal pancreas.

To study differences in cell morphology across these different cell lines, high-magnification confocal microscopy was employed to image cells two hours after the cells were in contact with the gel. After fixing and staining cells on a 2D collagen coated substrate, results from 2D fix and staining indicate that these cells do not form protrusions solely in the presence of 2D collagen coating (See Figure 19 A-H). Quantification of the number of microspikes that formed per cell for all of the different cell lines showed that MDA-MB-231, MEF, PAC001, U2OS, and PAC008 formed less than 10 spikes on average, while PAC009, PAC011, and HT1080 exhibited upwards of 40 microspikes (See Figure 20A).

When subjected to the invasion assay, the cells were divided into two different categories. As hypothesized, cells that showed drastically fewer microspikes per cell showed decreased rates of invasion. MDA-MB-231, MEF, U2OS, PAC001, and PAC008 showed very low rates of invasion, but on the other hand, at least 10% of PAC009, PAC011, and HT1080 cells invaded into the gel (See Figure 20B). In addition, the correlation between invasion and spike formation for the different cell lines showed a strong relationship between the two parameters. MDA-MB-231, MEF, U2OS, PAC001 and PAC008 all aggregated on the bottom left of the graph, while HT1080, PAC009 and PAC011 were all in a similar vicinity of the graph (See Figure 20C).

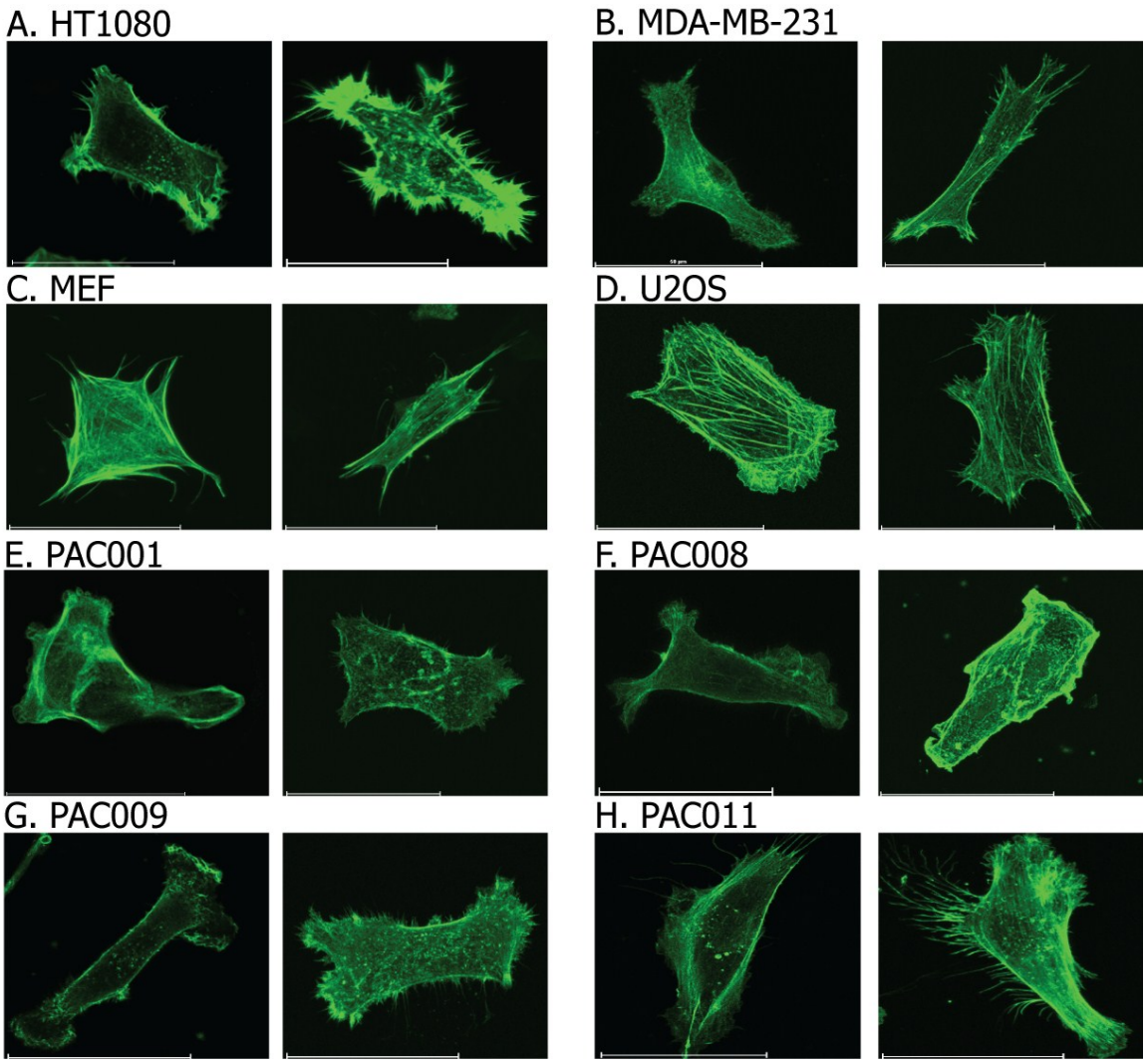

Figure 19: Images of Different Cell Lines in 2.5D and 2D. Cells in the 2.5D system were seeded for 24 hours on collagen-coated glass substrates and then fixed and stained for actin 2 hours after gelation for actin with phalloidin-488 (right image). Control cells plated on 2D collagen-coated glass for 24 hours and fixed and stained at the same time as the 2.5D samples (left image). With the external stimulus of a collagen gel, cells in 2.5D are much more elongated than cells adhered to a collagen coated substrate. **(A)** HT1080 cells. **(B)** MDA-MB-231 cells. **(C)** MEF cells. **(D)** U2OS cells. **(E)** PAC001 cells. **(F)** PAC008 cells. **(G)** PAC009 cells. **(H)** PAC011 cells. **(B-F)** does not exhibit spikes in a 2.5D system, while **(A, G, and H)** show a high quantity of spikes that form per cell.

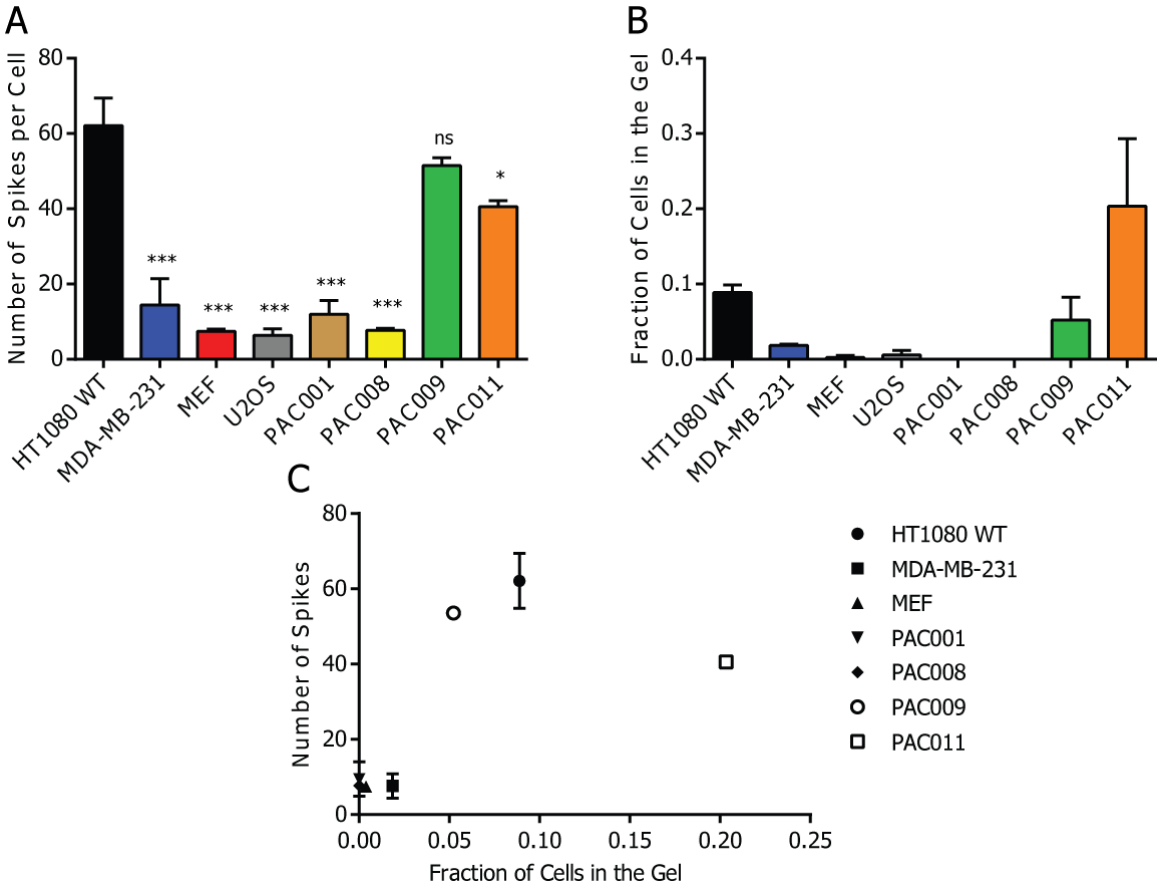

Figure 20: Microspike formation and invasion are correlated across different cell types. **(A)** Fraction of cells that invaded into the 2 mg/ml collagen gel for each cell line. After three days, MDA-MB-231, MEF, and U2OS show low rates of invasion while PAC001 and PAC008 do not invade at all. PAC009, PAC011, and HT1080 have at least 10% of cells that invaded into the gel. **(B)** Number of microspikes that formed per cell in response to the collagen gel for each cell line. MDA-MB-231, MEF, U2OS, PAC001, and PAC008 form fewer than 20 spikes on average. PAC009, PAC011, and HT1080 form upwards of 40 spikes, showing the drastic difference between the two different groups of cells. **(C)** Correlation between invasion and microspike formation per cell for different cell types. The cells that do not form microspikes and have low rates of

invasion or cannot invade at all are grouped on the bottom left corner of the graph. Cells that form upwards of 35 microspikes per cell and have higher rates of invasion lie to the right of the first group of cells.

DISCUSSION

Previous research shows that cells preferentially move towards stiffer substrates. Cells expand their lamellipodia and lamella as they approach rigid substrates while they retract their leading edge when they sense softer compositions (Wang et al., 2000). Here, we discovered that fibrosarcoma cells, including many other types of cells, adhered to a 2D collagen coated glass substrate show invasive capabilities in the presence of a 3D collagen gel stimuli. In the presence of a 3D environment, cells change their spread out morphology in response to the additional dimension, stimulated by the collagen fibers. When seeded in this 2.5D assay, the cells promptly reacted to its new microenvironment by forming long, thin microspikes that are present during the major physiological transformation of the cells. As cells stabilize in the 3D environment, the broad lamellipodia are replaced by thinner protrusions, and their overall morphology becomes more elongated. We hypothesized that these microspikes probe the environment and inform the cell that their surroundings have drastically changed. These signals may potentially lead to the reorganization of their cytoskeleton, transition of their overall morphology, and finally invasion.

Microspikes could also be correlated with other aspects of cancer cells. Shibue et al. have reported that filopodium-like protrusions (FLPs) help enable integrin-mediated adhesions between cells and the extracellular matrix following extravasation. The survival and proliferation after encountering a secondary tissue depends upon these adhesions, which are induced by EMT. Through testing various breast cancer cell lines with different metastatic potential in mice, they found that cell lines that could colonize in a foreign tissue formed a higher quantity of FLPs compared to cells that could not form

colonies. These results suggest that the ability to form FLPs determines the survivability of metastatic cells in a foreign tissue (Shibue et al., 2013).

To probe the mechanism underlying the invasion of cells into a 3D matrix from a 2D substrate, we investigated the behavior of cells in the 2.5D system over an extended period of time. Ranging from two to six days, the fraction of cells that invaded into the 3D matrix nearly doubled. Because the proliferation rates of cells at the 2.5D interface were higher than that of the cells that invaded into the gel, we can claim that this increase of cells in the gel is not due to the division of cells that had already migrated into the gel but is caused by the invasion of more cells. Another parameter we looked at was the farthest distance that the cells could travel through the gel. We used a diffusion-based model to rule out the possibility of simple diffusion is governing the transition of cells from a 2D monolayer to a 3D matrix, which suggested active cellular processes are involved in the 2D-3D transition process.

Furthermore, we explored the effects of cell density upon cell invasion. The strong dependence of invasion upon cell density could be related to collective migration. Previous work has shown that at high densities, leading cells can consume guidance cues, such as soluble factors, and sequester them from following cells. Transient physical contacts can equalize the differences among the group of cells; therefore, transient and stable contacts can equally cause cooperation in migration. Mesenchymal cells can collectively migrate and maintain the high cell density required for physical interactions. In tumors, collective migration can be promoted through the deformation of the surrounding tissues by tumor formation. Leading cells proteolytically degrade the extracellular matrix to invade further away from the primary tumor site. The room

created by these leading cells will increase the likelihood of cells' to migrate in larger groups. Another possibility is that the degradation uncovers previously hidden sites for cell-matrix adhesion (Treveneau et al., 2013).

By tuning the external properties of the 2.5D system, we attempted to investigate the effects of varying the mechanical properties of the microenvironment on the 2D-3D transition process. We used different concentrations of 3D collagen gels, ranging from 1 mg/ml to 4 mg/ml, to study whether stiffer gels with smaller pore sizes would hinder cell invasion. Invasion fractions of HT1080 cells did not decrease with higher collagen concentrations and remained relatively constant at all concentrations. These results suggest that fiber alignment and pore size of the collagen gel does not affect invasion for HT1080 cells. Additionally, we experimented with altering the mechanical properties of the substrate beneath the monolayer of cells. We used polyacrylamide gels to change the rigidity of the typically used glass plates. Surprisingly, the rates of invasion remained relatively constant over the three different conditions tested, suggesting that substrate stiffness does not play a role in the invasion of HT1080 cells.

To further study the mechanisms involved in invasion, we inhibited essential proteins involved in migration. Cells treated with marimastat and blebbistatin and depleted of β-1 integrin still retain their ability to invade at 1mg/ml, but with a smaller fraction of cells invading into the matrix. This signifies that invasion at this collagen concentration is not completely controlled by actomyosin contractions for migration, cell-ECM interaction , or matrix degradation. Since 1 mg/ml is the least dense concentration, cells may be able to migrate through the pores in the collagen mesh without the necessity to degrade the matrix. However, the cytoskeleton is indispensible for cells to transit into

1 mg/ml collagen matrix; at 1 mg/ml, cells could not invade without actin and microtubule intact.

Depletion of integrin and inhibition of MMPs, myosin II, actin, and microtubules almost completely block the transition of cells into 2 mg/ml and 4 mg/ml collagen matrix. The collagen gel's pore size decreases and may prohibit simple diffusion. Therefore, the invasion of cells into the 3D matrix are heavily dependent on cell-matrix interaction, actomyosin contractility and matrix digestion. The reduction of integrin eliminates the cell's ability to connect to its surroundings and communicate through outside-in or inside-out signaling. Without integrin to send messages either way, the cells cannot sense or bind to RGD peptides on collagen to generate enough traction for the cell and enough force to contract the matrix (Mierke et al., 2011) (Hood et al., 2002). Since the matrix is denser than 1 mg/ml MMPs must be secreted to degrade the ECM to provide enough room for cells to move. As illustrated above, cells need the cytoskeleton for any form of motility and it is conclusive that cells also lose their ability to invade in 2 mg/ml and 4 mg/ml concentrations of gel.

To further study the spikes' role in invasion, we investigated the properties of the spikes to uncover their identity. Previous research showed cells forming filopodia like protrusions (FLPs) when plated above a layer of Matrigel (Weinburg et al., 2013). Therefore, we assessed these microspikes to examine whether we discovered similar structures. We proved that the spikes were dependent on actin dynamics and did not rely on microtubule formation, which corresponds to previous work since most protrusions are composed mainly of actin (Ridley 2011). Following these results, we investigated the role of filopodia-related proteins in microspike formation and their potential role in

assembling microspikes. We used one fascin shRNA knockdown, and two shRNA knockdowns to ensure that the knockdowns were efficient for cdc42, β-1 integrin, and myosin X. We examined these proteins because of their importance in filopodia regulation. With the depletion of these crucial proteins, the cells still assembled microspikes at similar levels to HT1080 wild type. These results indicated that these microspikes were not filopodia because their assembly was independent of critical filopodia-associated proteins. In addition, we examined how cells invade into collagen gels and studied whether filopodia related molecules played a role in the transition from 2D to 3D. Cells depleted of fascin, cdc42, and myosin X showed no significant differences in the fraction of invasion over three days.

To investigate whether this transition was not unique to HT1080 cells or not, we studied a variety of widely used cell types originating from different cancers as well as noncancerous cells. We utilized MDA-MB-231, MEF, and U2OS cell lines, which are all extensively used in biomedical research. MDA-MB-231 is a human epithelial breast cancer cell derived from the metastatic site but is less invasive than HT1080. MEF cells are noncancerous fibroblasts that originate from the mouse, and U2OS cells are human epithelial osteosarcoma cells. We also included pancreatic cancer cell lines derived from patients obtained from Johns Hopkins pathology.

Through high-resolution confocal imaging and live-cell imaging, we determined that spike formation is required for invasion. Cells that showed a minimal amount of spikes (<20 spikes per cell), such as slightly invasive MDA-MB-231 and noncancerous MEF cells, showed low rates of invasion that correlated to *in vivo* behavior. Cells that exhibited high quantities of microspikes resulted in approximately 10% of cells invading

after three days. After analyzing the relationship between microspikes and invasion, we confirmed that there is a positive correlation between the number of microspikes that form per cell and the fraction of cells that invade for each cell line. The established correlation can help predict whether cell lines are invasive without the time consuming process of invasion and quantifying the fraction of cells that invade. The quantity of microspikes that assemble per cell two hours after the collagen gel is cast can be a quick indicator of whether cells can invade into a 3D matrix. This is an extremely helpful and powerful tool because the formation of microspikes has a much faster response time than waiting for the cells to reassemble their cytoskeleton, secrete MMPs, and finally begin invasion processes.

The transition observed in the 2.5D system under any of the conditions we experimented with is unexpected and truly a novel phenomenon. By ruling out most of the conventional modes of taxis that occur without any applied force, we hypothesized that we discovered a new form of taxis. Our experiments tested other modes of migration by creating a gradient of different properties to drive cell movement. As already explained, the invasion observed in this system is not durotaxis because the cells travel in the opposite direction of the rigidity gradient. Haptotaxis describes the movement of cells in attraction to cellular adhesion sites (Eccles et al., 2005). We accounted for this by saturating the wells with 2D collagen fibers as well as casting homogenous collagen gels. Other variables that could propel cells to invade are pore size, fiber alignment, and chemotaxis. Through varying the concentration of collagen in the 3D matrix, we determined that pore size and alignment do not play a role in cell invasion. Chemotaxis

is a possibility because media is added above the collagen gel after solidification and the nutrients above the gel may drive cells to move towards the media.

CONCLUSION

Our work here focuses on the morphological transition and invasion of cells from a 2D substrate to a 3D matrix. Our 2.5D assay provides a defined interface between the substrate and the gel, which makes it possible to observe the transition process of cells from 2D into 3D matrix. We were also able to obtain high-resolution images of cells transforming in the presence of the collagen gel. We observed that one of the first steps in 2D to 3D transition is the formation of thin microspikes lining the cell body, which are present as the cells' broad lamellipodia transform into elongated protrusions. These microspikes may function as one of the first steps for invasion, acting as explorers for the cell to sense that their environment has changed.

To determine the factors involved in invasion, we presented that external properties of the cell microenvironment do not affect invasion for HT1080 by altering the concentration of the collagen gel and the stiffness of the substrate beneath the cells. Cell density is a powerful factor upon invasion rates and highest distance that cells travelled. Upon increasing the cell density, both parameters increased in an exponential rate. This phenomenon is extremely interesting because intracellular signaling appears to play a huge role in invasion processes. This led us to explore additional proteins that are required for cytoskeleton dynamics, cell migration, and ECM communication. Results suggest that in a soft collagen gel at a concentration of 1 mg/ml, cells can potentially invade independently of MMPs, myosin II and β-1 integrin; however, invasion is hindered in denser collagen gels without the function of MMPs, myosin II, β-1 integrin, actin, and microtubules.

Based on Shibue's work and our initial hypothesis that these microspikes were similar to filopodia, we studied the function of key proteins involved in filopodia regulation to uncover the microspikes' properties. However, we were not able to establish any type of relationship between the deletion of these proteins and quantity of microspikes, indicating that these proteins did not play a role in microspike assembly. By investigating the internal properties that control cell invasion, we showed that the filopodia related proteins did not affect invasion rates. Both of these conclusions signify that these microspikes are most likely not filopodia.

We finally showed that these spikes were not exclusive to HT1080 cells by testing multiple cell lines in this system. We confirmed that these spikes are a response to the collagen gel by gathering images of cells after collagen gel casting that were initially adhered to a 2D collagen gel. Furthermore, we established a positive correlation between the quantity of microspikes that formed in the cells after collagen casting and the fraction of the cells invading into the gel. This relationship can be used to quickly assess whether a specific cell type can invade when stimulated by a 3D matrix instead of conducting our invasion assay, which can take up to a week to obtain results.

FUTURE WORK

For future work, we will use a different cell line to observe effects upon varying external properties in this system. Based upon initial results, changing the collagen gel concentration above the cells and the substrate rigidity below the cells did not affect the fraction of cells that invaded into the gel. However, previous work has shown that the mechanical properties of the microenvironment do affect the invasion of cells (Griffth et al., 2011). To reveal if these results are unique to HT1080 because of their high invasive capabilities, we will use metastatic human breast cancer epithelial cells, MDA-MB-231, to repeat these experiments.

We propose to further investigate the different signaling pathways that may be involved in spike formation. Since we have already concluded that these microspikes are not filopodia, our next step is to use key molecules involved in the formation of invadopodia. We plan to target the Arp2/3 complex, N-WASP, and mDia formins, which are all required for invadapodia assembly. Another protein of interest is filaminin, a crosslinking protein that stabilizes bundles of actin (Ridley 2011). Integrating the shRNA technique and the 2.5D system, we will investigate whether these proteins are necessary for microspike assembly and whether these structures are similar to invadapodia.

In addition to the fixed and stained images two hours after casting the collagen gel, we want to have a more complete picture of what is truly happening as the cell invades, which will help us understand how these microspikes contribute to invasion. To help guide us, we will take high-resolution images of the morphology of cells at the 2.5D interface and in the gel three days after collagen gel casting. Our hypothesis is that after three days, more cells at the interface will be preparing to invade and show transient

morphology that we have not captured yet. We also want to analyze the cytoskeleton of the cells that have already invaded into the gel and see whether the microspikes are still present in cells that have stabilized in their new environment. This will help us conclude whether the microspikes are temporary structures and function solely to help initiate invasion. All of these snapshots will provide a better comprehension of the involvement of microspikes in the transition from 2D to 3D.

REFERENCES

Alberts, Bruce. *Molecular Biology of the Cell.* New York: Garland Science, 2008.

Arjonen, A., R. Kaukonen, et al. (2011). "Filopodia and adhesion in cancer cell motility." Cell Adhesion & Migration **5**(5): 421-430.

Bohil, A. B., B. W. Robertson, et al. (2006). "Myosin-X is a molecular motor that functions in filopodia formation." Proc Natl Acad Sci U S A **103**(33): 12411-12416.

Brekhman, V. and G. Neufeld (2009). "A novel asymmetric 3D in-vitro assay for the study of tumor cell invasion." BMC Cancer **9**: 415.

Chambers, Ann F. and L. M. Matrisian (1996). "Changing views of the role of matrix metalloproteinases in Metastasis." Journal of the National Cancer Institute **89**(17). 1260-1270.

Cheney, RE, AB Bohil, et al. (2006). "Myosin-X is a molecular motor that functions in filopodia formation." PNAS **103** (33): 12411-12416.

Clark, J. C., C. R. Dass, et al. (2008). "A review of clinical and molecular prognostic factors in osteosarcoma." J Cancer Res Clin Oncol **134**(3): 281-297.

Cooper, John A., T. D. Pollard. (2009). "Actin, a central player in cell shape and movement." Science **326**: 1208-1212.

Deisboeck, T. S. and I. D. Couzin (2009). "Collective behavior in cancer cell populations." Bioessays **31**(2): 190-197.

Eccles, S. A., C. Box, et al. (2005). "Cell migration/invasion assays and their application in cancer drug discovery." Biotechnol Annu Rev **11**: 391-421.

Egeblad, M. and Z. Werb (2002). "New functions for the matrix metalloproteinases in cancer progression." Nature Reviews Cancer **2**(3): 161-174.

Even-Ram, S. and K. M. Yamada (2005). "Cell migration in 3D matrix." Current Opinion in Cell Biology **17**(5): 524-532.

Felder, RA, BA Justice, et al. (2009). "3D cell culture opens new dimensions in cell-based assays." Drug Discovery Today **14**: 102-107.

Friedl, P. and S. Alexander (2011). "Cancer invasion and the microenvironment: plasticity and reciprocity." Cell **147**(5): 992-1009.

Fuster, Mark M. and Jeffrey D. Esko (2005). "The sweet and sour of cancer: glycans as novel therapeutic targets." Nat Rev Cancer **5**:526-542.

Guillou, H. et al. Lamellipodia nucleation by filopodia depends on integrin occupancy and downstreamRac1 signaling. Exp. Cell Res. 314, 478–488 (2008).

Griffith, L. G. and M. A. Swartz (2006). "Capturing complex 3D tissue physiology in vitro." Nat Rev Mol Cell Biol **7**(3): 211-224.

Hakkinen, K. M., J. S. Harunaga, et al. (2011). "Direct comparisons of the morphology, migration, cell adhesions, and actin cytoskeleton of fibroblasts in four different three-dimensional extracellular matrices." Tissue Eng Part A **17**(5-6): 713-724.

Hayden, J. B. and B. H. Hoang (2006). "Osteosarcoma: basic science and clinical implications." Orthop Clin North Am **37**(1): 1-7.

Hood, J. D. and D. A. Cheresh (2002). "Role of integrins in cell invasion and migration." Nature Reviews Cancer **2**(2): 91.

Justice, B. A., N. A. Badr, et al. (2009). "3D cell culture opens new dimensions in cell-based assays." Drug Discov Today **14**(1-2): 102-107.

Kam, Y., C. Guess, et al. (2008). "A novel circular invasion assay mimics in vivo invasive behavior of cancer cell lines and distinguishes single-cell motility in vitro." BMC Cancer **8**: 198.

Kramer, N., A. Walzl, et al. (2013). "In vitro cell migration and invasion assays." Mutat Res **752**(1): 10-24.

Lo, C. M., H. B. Wang, et al. (2000). "Cell movement is guided by the rigidity of the substrate." Biophys J **79**(1): 144-152.

McCarthy, JB, Palm SL, Furcht LT. (1983). “Migration by haptotaxis of a Schwann cell tumor line to the basement membrane glycoprotein laminin”. J Cell Biol **97** (3) 772-777.

Mierke, C. T. (2013). "Physical break-down of the classical view on cancer cell invasion and metastasis." Eur J Cell Biol **92**(3): 89-104.

Nguyen, D. X., P. D. Bos, et al. (2009). "Metastasis: from dissemination to organ-specific colonization." Nature Reviews Cancer **9**(4): 274-284.

Nurnberg, A., T. Kitzing, et al. (2011). "Nucleating actin for invasion." Nature Reviews Cancer **11**(3): 177-187.

Pollard, T. D. and J. A. Cooper (2009). "Actin, a Central Player in Cell Shape and Movement." Science **326**(5957): 1208-1212.

Pouliot, N., H. B. Person, et al. (2000). “Investigating Metastasis Using In Vitro Platforms.” Metastatic Cancer: Clinical and Biological Perspectives

Ridley, A. J. (2011). "Life at the Leading Edge." Cell **145**(7): 1012-1022.

Sahai, E. (2005). "Mechanisms of cancer cell invasion." Curr Opin Genet Dev **15**(1): 87-96.

Shibue, T., M. W. Brooks, et al. (2013). "An integrin-linked machinery of cytoskeletal regulation that enables experimental tumor initiation and metastatic colonization." Cancer Cell **24**(4): 481-498.

Steeg, P. S. (2006). "Tumor metastasis: mechanistic insights and clinical challenges." Nat Med **12**(8): 895-904.

Theveneau, E. and R. Mayor (2013). "Collective cell migration of epithelial and mesenchymal cells." Cellular and Molecular Life Sciences **70**(19): 3481-3492.

Vignjevic, Danijela, S. Kojima et al. (2006). "Role of fascin in filopodial protrusion." The Journal of Cell Biology **174**(6): 863-875.

Wolf, K., S. Alexander, et al. (2009). "Collagen-based cell migration models in vitro and in vivo." Semin Cell Dev Biol **20**(8): 931-941.

Yu, X. and L. M. Machesky (2012). "Cells assemble invadopodia-like structures and invade into matrigel in a matrix metalloprotease dependent manner in the circular invasion assay." PLoS One **7**(2): e30605.

Zimmermann, M., C. Box, et al. (2013). "Two-dimensional vs. three-dimensional in vitro tumor migration and invasion assays." Methods Mol Biol **986**: 227-252.

Angela San

10322 Nolan Drive • Rockville, MD 20850 • asan730@gmail.com • Cell: (908) 458-1189

Education

Johns Hopkins University – Baltimore, MD — Expected May 2014
Master of Science in Engineering in Chemical and Biomolecular Engineering — **Cumulative GPA:** 3.94

Johns Hopkins University – Baltimore, MD — August 2009 – May 2013
B.S. in Chemical and Biomolecular Engineering — **Cumulative GPA**: 3.76, **Major GPA**: 3.91
Relevant Coursework: Modeling Dynamics and Control, Modeling and Statistical Analysis, Chemical Engineering Product and Process Design, Chemical and Biomolecular Engineering Lab, Professional Communication for Business, Science and Industry, and Case Studies in Business Ethics

Professional Experience

Graduate Student Liaison Committee – — September 2013 – Present
Professional Development Committee, Baltimore, MD

- Plan informational sessions on how to successfully attain a job in academia or industry for graduate students by partnering with the Johns Hopkins Career Center
- Coordinate with industry professionals, faculty, and alumni to host panel events to share experiences and network
- Host poster sessions including all laboratories within the department to educate students about other research

Chemical Engineering Product Design – — January – May 2013
Team Member, Baltimore, MD

- Served as a leader during design development and provided guidance to team members necessary to meet goals
- Presented our product design, market analysis, and financial analysis to a diverse professional audience
- Designed an oral spice relieving strip by researching product components and production methods
- Modeled the dissolving rate profile by applying the Baker-Lonsdale Model, a mathematical drug release model
- Submitted proposal memos throughout the design process and a formal product design report

W.R. Grace – *Chemical Engineering Intern*, Baltimore, MD — June – August 2012

- Determined target values and limits on control devices of emission points and reporting requirements for The Clean Air Act
- Collaborated with plant superintendents and production engineers to implement new procedures for safety inspections of plant equipment
- Organized data collection processes for control variables to follow The Clean Air Act regulations

Research Experience

Wirtz Lab at Johns Hopkins – *Graduate Student Researcher* January 2013 – Present
Baltimore, MD

- Design experiments to investigate the morphological and mechanistic changes that occur when cells invade from 2D substrates to 3D matrixes
- Analyze the transition efficiency of cells by varying properties of this system
- Mentor and train undergraduate students in cell culture techniques, data analysis, and microscopy

Ostermeier Lab at Johns Hopkins – *Research Assistant* January – August 2011
Baltimore, MD

- Developed gene variants of a linker region in an engineered protein switch
- Analyzed how specific amino acids in the linker region affected the stability and activity of the protein switch
- Discovered that the length of the linker region has a significant effect on the protein switch's activity

Awards and Honors

- JHU Chemical and Biomolecular Engineering Award of Excellence in Academics received Spring 2013
- Tau Beta Pi, Professional Engineering Honor Society, Maryland Alpha Chapter inducted Fall 2013
- JHU Chemical Engineering Product Design Award: Best Product Design and Best Engineering Knowledge – 2013
- JHU Whiting School of Engineering Dean's List received Fall 2010, and Fall & Spring: 2011, 2012, 2013

Publications

Choi, J. H., **A. San**, and M. Ostermeier. "Non-allosteric enzyme switches posses larger effector-induced changes in thermodynamic stability their non-switch analogs." *Protein Science,* Volume 22*,* Issue 4, Pages 475-485.

Skills

Computer: MatLab, NIS Elements Advanced Research, Microsoft Excel, Windows and Macintosh OS